



Calhoun: The NPS Institutional Archive
DSpace Repository

Theses and Dissertations

1. Thesis and Dissertation Collection, all items

1966

Aeroelastic problems in an antenna vibration project.

Mortenson, W. P.

Monterey, California. U.S. Naval Postgraduate School

<http://hdl.handle.net/10945/9428>

Downloaded from NPS Archive: Calhoun



Calhoun is the Naval Postgraduate School's public access digital repository for research materials and institutional publications created by the NPS community. Calhoun is named for Professor of Mathematics Guy K. Calhoun, NPS's first appointed -- and published -- scholarly author.

Dudley Knox Library / Naval Postgraduate School
411 Dyer Road / 1 University Circle
Monterey, California USA 93943

<http://www.nps.edu/library>

NPS ARCHIVE
1966
MORTENSON, W.

AEROELASTIC PROBLEMS IN AN
ANTENNA VIBRATION PROJECT

WILLIAM PETER MORTENSON

rary
S. Naval Postgraduate School
Monterey, California

DUDLEY KNOX LIBRARY
NAVAL POSTGRADUATE SCHOOL
MONTEREY CA 93943-5101

This document has been approved for public
release and sale; its distribution is unlimited.

AEROELASTIC PROBLEMS IN AN
ANTENNA VIBRATION PROJECT
by

William Peter Mortenson
Lieutenant, United States Navy
B.S., United States Naval Academy, 1958



Submitted in partial fulfillment
for the degree of
AERONAUTICAL ENGINEER
from the
UNITED STATES NAVAL POSTGRADUATE SCHOOL
May 1966

NPS Archive
1966
Mortenson, W

~~TOP SECRET~~
~~SECRET~~

ABSTRACT

Continued studies were made of bluff-body separation and its effect upon the response of an aeroelastic model for a range of tunnel air speeds and model cross sections. The motivation for this work was the application to the antenna-element vibration problem as posed in the various Wullenwebber type antenna installations operated by the United States Navy throughout the world.

A retrofit configuration change was devised to significantly decrease the wind-induced response of the long horizontal "boom boards". Although flow separation still exists, the character of the aerodynamic forcing function has been modified such that the energy spectra have apparently been broadened from a single dominant peak into many weaker peaks. Thus the effective total response is reduced.

The digital data processing has been extended in scope due to the repeatability in signal analysis. Estimates have been made of the "two-dimensional" random input forcing function using the output response in conjunction with the aeroelastic-model transfer function. Reasonably good results were obtained and an estimate was made of the root-mean-square value of the unsteady fluctuating air load.

TABLE OF CONTENTS

Section	Page
1. Introduction	11
2. Test Description	13
3. Scaling	15
4. Antenna Applications	18
H/D Ratio	18
Corner Radii	18
Gloves	19
Circular Cylinder	21
5. Estimate of Unsteady Lift	23
6. Summary	29

LIST OF TABLES

Table	Page
I. Run Schedule	31
II. Scaling Study Calculations, Square Cross Section	34
III. H/D Calculation	35

LIST OF ILLUSTRATIONS

Figure	Page
1. Antenna installation general layout	36
2. Typical boom board cross sections	37
3. Spring bar calibration	38
4. Dynamic response, square cylinder	39
5. Effects of motion on lift, square cylinder	40
6. Effects of H/D ratio, $l_B = 3$ inches	41
7. Effects of H/D ratio, $l_B = 3$ inches	42
8. Bluff body drag summary	43
9. Model cross sections	44
10. Effects of corner radii on dynamic response	45
11. Glove geometry	46
12. Effects of gloves, $l_B = 6.5$ inches	47
13. Effects of glove on 5.7-inch square, $l_B = 6.5$ inches	48
14. Effects of glove on 5.7-inch square, $l_B = 5.0$ inches	49
15. Effects of glove on 4.0-inch square, $l_B = 6.5$ inches	50
16. Effects of glove on 4.0-inch square, $l_B = 5.0$ inches	51
17. Circular cross section, shroud fairings	52
18. Effects of shroud fairings, circular cylinder, $l_B = 3.0$ inches	53
19. Effects of shroud fairings, circular cylinder, $l_B = 6.5$ inches	54
20. PSD output $q = 8$ psf	55
21. PSD output $q = 40$ psf	56
22. Coefficient of lift, experimental results	57
23. Coefficient of lift, data summary	58
24. PSD input $q = 8$ psf	59
25. PSD input $q = 40$ psf	60
26. Aeroelastic effects on unsteady lift	61

TABLE OF SYMBOLS

D	- model depth
f	- frequency (cycles per second)
f_n	- natural frequency
H	- model frontal width
I	- mass moment of inertia of model relative to pivot axis
l_B	- length of spring rod (inches)
m	- mass (slugs)
q	- test section dynamic pressure, $\frac{1}{2} v^2$, (psf)
R/H	- ratio of glove radius to length of side of square
Re	- Reynolds number = Vh/ν
S	- Strouhal number
V	- velocity
$Z(i\omega)$	- complex impedance
β	- damping ratio, fraction of critical
ρ	- density of test section air, (slugs/ft ³)
ν	- kinematic viscosity

Note: Symbols associated with a particular derivation are defined when first used in text.

1. Introduction.

A bluff body may be defined from an aerodynamic sense as a body whose drag forces are primarily due to pressure or form drag. The airflow does not progress smoothly around the body, but instead separates randomly and defines a turbulent flow region. As a consequence of the flow separation, fluctuating pressures or air loads are generated which can be resolved into unsteady air load components in both the lateral (lift) and stream-wise (drag) directions. In general, the fluctuating lift forces dominate and give rise to the most significant vibration modes.

Physical structures are elastic and consequently will respond to dynamic air loads that are wind generated. Examples of the response of bluff bodies to unsteady air loads are frequently observed in every day events, examples of which would include the galloping transmission line problem, vibrating telephone wires, smokestack motion, ground-wind loads on missiles, and vibrating-antenna elements. There are many other situations of structural shapes responding to wind-induced air loads.

It was the purpose of this study to investigate the bluff-body problem with particular application to an important element of a large antenna (Wullenwebber^{type}) system that is currently in use by the United States Navy. The basic arrangement includes a number of towers located in a circular pattern. Figure 1 shows a pair of towers supporting a horizontal boom board. The boom boards extend around the entire circle, and serve the function of supporting vertical reflecting wires. The boom boards are 28 to 56 feet long (depending on the installation) and are approximately 100 feet above the ground. There have been instances reported of large amplitude motion of boom boards which were directly exposed to the airflow, and even some instances of component failures.

An important consideration in this study is that the cross sections used for the boom boards are not the same for every installation since it is the option of each contractor to perform the detail design. Figure 2 is a sketch showing the basic cross sections used for the boom boards. Only one installation (Winter Harbor, Maine) employs the circular cross section. There are three basic types of rectangular cross sections. The solid laminated boom board is used in three general sizes. The hollow square and the inverted "U" are lighter per unit cross section area, but lack the strength of solid construction. The inverted "U" does have

short lengths of wood across the bottom which support the vertical wires and provide structural support to maintain the shape.

In order to fulfill the objectives of this study, it was desirable to:

- (1) Gain an insight into the factors influencing the response of a simulated aeroelastic bluff body.
- (2) Determine possible fixes suitable for application to the actual antenna installation.
- (3) Attempt to estimate the character and magnitude of the aerodynamic input.

This work has been sponsored by the Structures Division of the United States Naval Civil Engineering Laboratory (USNCEL), Port Hueneme, California under work request WR 600028, dated 23 August 1965.

The investigation was conducted with Lieutenant R. H. Jesberg, U. S. N. Tests were conducted in the West Coast Research Corporation (W.R.C.) low-speed wind tunnel located in Building 234 at the United States Naval Postgraduate School, Monterey, California. For detailed information on equipment and data handling procedures used in this study, see "Data Handling Procedures in Support of the Study of Aeroelastic Problems in an Antenna Vibration Project" by Lieutenant R. H. Jesberg, U. S. N. [7].

Sincere appreciation is extended to faculty and staff of the Department of Aeronautics for assistance and support which was vital to the success of this investigation. The author is indebted to Associate Professor L. V. Schmidt for his invaluable counseling and guidance.

2. Test Description.

An aeroelastic bluff body model was installed to vertically span the 3.5 x 5.0-foot test section of the W.R.C. low-speed wind tunnel. The wind tunnel is of the continuous flow type, and has an atmospheric vented test section. Test parameters included tunnel dynamic pressure (q), model cross-section geometry, and model natural frequency (f_n).

The cross section of the model was altered by fitting various shapes of balsa wood on an aluminum I beam. The low density of balsa wood made it possible to make changes in cross-section geometry without significantly altering the weight, center of gravity, and mass moment of inertia of the complete model.

The aluminum I beam was flexurally supported at the top (outside of the test section) and could move laterally in response to the unsteady-lift loads. A drag constraint was provided at the lower end by a simple drag cable support. The natural frequency of the lateral motion was controlled by adjusting the length of a spring rod (l_B) attached at the base of the I beam. Figure 3 presents the variation of model resonant frequency with spring rod length. Extreme care was used in the design of model components in order to assure repeatability of results and the avoidance of model slippage.

For information on the complete design of the aeroelastic model used to represent the antenna boom boards, see Jesberg [7]. Included in [7] is a description of the displacement transducer used to measure lateral motion at the model base, the data handling and tape recording systems, the method used to convert analog to digital data, and the digital computer program employed to convert voltage time history into auto-correlation and power spectral density forms.

A listing of the run schedule is provided in Table I. Runs 22 through 45 were part of the first phase of testing and took place during the period of 22 October to 2 November 1965. The objectives of the first phase may be stated as:

<u>RUN</u>	<u>OBJECTIVE</u>
20 to 27	Familiarization and check out of test set-up with square and circular cylinders.
28 to 30	Check the effect of rounding the corners on a square.

31 to 36 Investigation of miscellaneous configurations.

37 to 45 Check the effect of rounding the corners on a square.

The natural frequencies used in phase one were 36, 42, and 82 cycles per second (cps) which corresponded to beam lengths of $l_B = 6.5, 5.0,$ and 3.0 inches respectively. Upon completion of the first phase of testing, the data that had been recorded on magnetic tape were reexamined. Frequencies of all indicial response checks and tunnel test data were confirmed by plotting a portion of the tape data playback onto an ink recording oscillograph.

Following phase one, modifications were made in order to improve data acquisition and reliability. The spring rod support bracket was redesigned for ease of setting spring rod length and for improvement of spring rod constraint. The displacement sensor was relocated to the centerline of the aluminum I beam. In addition, the spring rod was case hardened.

The second phase of these investigations began with run 46 on 24 January and continued through run 84 on 25 February 1966. The objectives for this phase of the program were:

<u>RUN</u>	<u>OBJECTIVE</u>
46 to 51	Check the effects of modifications and compare results with first phase data.
52 to 62	Check shroud for retrofit on currently installed boom boards.
63 to 74	Check scaling laws and effects of H/D ratio.
75 to 77	Check feasibility of using a shroud on flanges of the circular boom board.
78 to 84	Investigate the forcing function.

The natural frequencies used during this phase were different due to the equipment modifications that took place between the first and second phases. The three basic natural frequencies used were 55, 70, and 89 cps, which corresponded to l_B values of 6.5, 5.0, and 3.0 inches respectively.

3. Scaling.

Accurate scaling of a wind-tunnel model is a fundamental consideration in establishing an experimental program. Important variables involved in an aeroelastic simulation include fluid density, viscosity, velocity, model vibration frequency, stiffness, and mass distribution. Since the model was restricted to a single degree of freedom (in the lateral direction), the moment of inertia did not have to be scaled.

All essential scaling variables are included in either Reynolds number ($Re = VH/\nu$) or Strouhal number ($S = fH/V$). The Reynolds number of the model and prototype were matched to assure that the aerodynamic-forcing functions corresponded. All models were operated at values of Reynolds number between 250,000 and 750,000. The full-scale antenna element with a frontal width of one foot would have a Reynolds number of 700,000 for a wind velocity condition of 75 miles per hour (mph) at sea level.

Strouhal number is the dimensionless vortex-shedding frequency of the air flow and a match of this number assures a correspondence between the model and the prototype dynamic response. In general the prototype-antenna elements have a natural frequency of about five cycles per second; and as suggested by USNCEL personnel, a dynamic matching should correspond to a wind velocity of about 75 mph on a beam with approximately one-foot frontal width. At the design point, the fundamental structural Strouhal number is about 0.05. Since the model indicated large amplitude responses at $S = 0.14$ and multiples above, it is unlikely that the boom-board natural frequencies could act to reinforce the amplitude response at wind velocities above about 30 mph.

It is customary to present wind tunnel results in the form of dimensionless coefficients, i.e., lift coefficient (C_L), drag coefficient (C_D), etc. In contrast the dynamic responses reported here are not normalized and in general it will be necessary to make relative comparisons to see improvements or changes due to configuration revisions.

It is interesting to check for dynamic matching since a good indication of dynamic model characteristics can be obtained. Figure 4 has been arranged to show the lateral response of the model for the case of a square cross section. Parameters shown in Figure 4 include model size (H) and spring rod length (l_B). A casual glance shows that shortening

the spring rod reduces the dynamic response, but decreasing the frontal width does not consistently decrease the motion amplitude. Therefore, comparisons can be made only when taking into account the scaling parameters.

It can be shown that the root-mean-square (R.M.S.) of the lateral response is proportional to the expression below for a single degree of freedom model:

$$\sqrt{y^2} \sim \sqrt{\bar{C}_L^2} \frac{q H L^3}{I} \left\{ \int_0^\infty \frac{\Phi_i(f) df}{(2\pi f_n)^4 \left[\left[1 - \left(\frac{f}{f_n} \right)^2 \right]^2 + 4 \beta^2 \left(\frac{f}{f_n} \right)^2 \right]^2} \right\}^{1/2} \quad (1)$$

where:

y - lateral response at the lower end of the model

H - beam frontal width

L - beam exposed frontal length

I - system mass moment of inertia about the flexure pivot

f - frequency, cps

\bar{C}_L^2 - mean square of the fluctuating lift, assumed to be uniform over model length

Φ_i - spectral density of input aerodynamic forcing function

Now by a basic definition,

$$\bar{C}_L^2 = \int_0^\infty \Phi_i(f) df = \int_0^\infty \Phi_i(s) ds \quad (2)$$

Equation 2 provides a scaling relation when Φ is expressed in terms of density with respect to either frequency or Strouhal number. Since $f/f_n = S/S_n$ at a given operating condition, the scaling law is:

$$\frac{\sqrt{y_1^2}}{\sqrt{y_2^2}} = \frac{\sqrt{\bar{C}_{L1}^2}}{\sqrt{\bar{C}_{L2}^2}} \frac{q_1 H_1}{q_2 H_2} \left(\frac{f_{n2}}{f_{n1}} \right)^2 \quad (3)$$

This law holds providing that $I_1 = I_2$ and $[\Phi_i(s)]_1 = [\Phi_i(s)]_2$.

If the Reynolds number effect can be neglected and if there were no aeroelastic feedback dependence, then one could assume $\sqrt{\bar{C}_{L1}^2} = \sqrt{\bar{C}_{L2}^2}$.

On this basis equation 3 will simplify further to:

$$\frac{\sqrt{y_1^2}}{\sqrt{y_2^2}} = \frac{q_1 H_1}{q_2 H_2} \left(\frac{f_{n2}}{f_{n1}} \right)^2 \quad (4)$$

Comparison again will be made using the data on Figure 4 under the assumption of matching Strouhal numbers. The steady-state drag data as shown on Figure 8 lead to the assumption that Reynolds number effects are relatively unimportant for a sharp-edged square or rectangular cross section. The starting point for the comparison is from run 58 at $q = 20$ psf. The reference values are listed in Table II, part A. In making a ratio comparison, the response with the smallest displacement value (case c) will be used as a reference. On this basis, calculations were made and are listed in Table II, part B. It will be noted that the ratios of R.M.S. displacements do not agree with the ratios based upon q , H , and f_n , but in all cases the displacement ratios were larger. A glance at equations 3 and 4 immediately points out that the assumption of constant $\sqrt{C_L}$ as assumed in equation 4 is probably not valid. Column 3 in Table II, part B is the ratio showing the discrepancy and has the physical interpretation of being the increase in $\sqrt{C_L}$ due to aeroelastic feedback or dynamic motion.

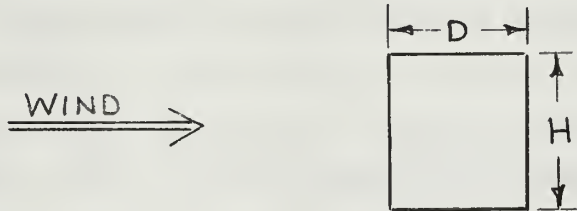
Figure 5 is a plot showing the apparent increase in fluctuating lift due to motion. The abscissa represents lateral motion normalized with respect to frontal width. The data points are the values obtained from Table II, part B and all values are in reference to an elastic condition. A simple rotation of the curve, so that with zero motion the ordinate has a value of unity, provides an estimate of the lift increase due to aeroelastic feedback. It should be noted that in estimating this curve, no information has been obtained as to the magnitude of the fluctuating lift.

A later section of this paper will deal with estimating the fluctuating lift and an account will be given to aeroelastic feedback again. In the discussion to follow concerning cross sections applicable to the antenna problem, only relative comparisons will be made.

4. Antenna Applications.

H/D Ratio

All but one of the boom-board cross sections for the Wullenweber antennas are rectangular in shape. The H/D ratio varies from one to two and a half.



A series of runs were conducted in order to demonstrate the influence of varying D while holding H constant. The three beams selected for this evaluation were:

- (1) 6.0 x 3.0-inch rectangle ($H/D = 2.0$)
- (2) 6.0 x 4.0-inch rectangle ($H/D = 1.5$)
- (3) 5.7 x 5.7-inch square ($H/D = 1.0$)

The small error introduced when using the 5.7-inch square was considered acceptable since the values used for comparison were corrected to similar values of Strouhal number.

The responses for natural frequencies of 89 and 70 cycles per second are shown on Figures 6 and 7. Table III is the numerical results of the H/D ratio study. It will be noted that the amplitude response is approximately inversely proportional to the H/D ratio (holding H constant).

The physical meaning of these results is that the fluctuating pressures acting over the lateral faces of the bluff body are primarily controlled by the corners and not the width of the lateral faces.

Corner Radii

A frequent statement made for circular cylinders is that the unsteady lateral air load is of the same order of magnitude as the steady state drag while the unsteady drag is an order of magnitude less. Using this as a clue, insight into the behavior of circular, square, and rectangular cross sections may be gained by looking at Figure 8 which is a summary of a drag study made by Delany and Sorensen [3]. The square cylinder does not show a drag transition trait as for a circular cylinder for Reynolds number values well beyond 1×10^6 . However, placing a radius on the corner

edges does bring a transition trait into being. Since the circular-cross-sectioned aeroelastic model was relatively more docile than the square cross-section,,the material of Delany and Sorenson provided the motivation to try corner radii.

Figure 9 shows a series of cross sections that gradually transform the square cylinder to a circular cylinder. The corners of the 5.7-inch square were successively rounded in one-half-inch increments of radius up to and including a two-inch radius. This series of cross sections transformed the square cylinder into a circular cylinder in definable steps. It was anticipated that rounding the corners of a square would produce responses that fall between the responses of the square and circular cylinders.

Typical results obtained are the responses for a model with a three inch spring rod length as shown in Figure 10. The curve farthest to the left, is the response for a square and it will be noted that the response rapidly exceeds the limit of the graph. The addition of one-half-inch radius corners ($R = 0.5$ inch) on the 5.7-inch square ($H = 5.7$ inch) results in some improvement ($R/H = 0.0877$). The one-inch radius ($R/H = 0.176$) shows marked improvement. The one and a half-inch radius ($R/H = 0.263$) exhibited a low amplitude response characteristic and the two-inch radius ($R/H = 0.351$) was comparable to the circular cylinder.

The advantages that can be obtained by rounding the corners of the boom boards are obvious when looking at Figure 10. The solid laminated boom boards would be particularly well adapted to this fix. However the boom boards with hollow centers would be seriously weakened if the corners were rounded.

$R/H = 0.263$ is suggested for the construction of new boom boards. However, a corner radius ratio of $R/H = 0.176$ would provide a considerable improvement over the square corners which are now being used.

Gloves

Rounding the corners of a rectangular beam provided well defined decreases in lateral amplitude response of the beam. There are two reasons that discourage the use of this fix on the currently installed boom boards. First, all boom boards that are hollow in the center would be seriously weakened if the corners were rounded. Secondly, the boom boards are physically located 100 feet above the ground. It would be

easier to install some additional piece of material to a beam than remove part of the beam.

A shroud on the corners of a square was selected as a possible fix. Figure 11 is a sketch of this shroud or glove as it will be referred to in this paper. From the results of an earlier series of tunnel runs where the corners of a square were rounded in successive one-half-inch increments, a ratio $R/H = 0.22$ was selected for the glove. The square with a two-inch radius ($R/H = 0.351$) had the most effect in reducing the dynamic response when compared with the basic square cross section. However, a glove with an R/H ratio of 0.351 would be relatively large, thus greatly increasing the weight and frontal area of the beam. A compromise was made in selecting a glove radius so that undue penalties in frontal area and weight addition would not take place, while still providing the benefits of reducing dynamic response of the boom boards.

Two sets of gloves ($R = 0.875$ inches and $R = 1.25$ inches) were constructed to be used with two squares ($H = 4.0$ inches and $H = 5.7$ inches). This provided four possible configurations with gloves to check for possible scaling laws and to give some indication of a desirable R/H ratio.

- (1) 5.7-inch square with 1.25 -inch gloves ($R/H = 0.22$)
- (2) 5.7-inch square with 0.875-inch gloves ($R/H = 0.15$)
- (3) 4.0-inch square with 1.25 -inch gloves ($R/H = 0.31$)
- (4) 4.0-inch square with 0.875-inch gloves ($R/H = 0.22$)

Configuration (2) would indicate if the R/H ratio selected were too large. Configuration (3) would likewise indicate if the R/H ratio were too small. All four configurations have been plotted in Figure 12 for a spring rod length of six and one half inches ($f_n = 55$ cps). All curves exhibited considerable improvement over the response of the square cross section.

Figures 13 and 14 show the response of the 5.7-inch squares with and without gloves. A ratio of $R/H = 0.22$ has a clear advantage of a lower response below a dynamic pressure of 30 pounds per square foot. When a natural frequency of 55 cps was used the $R/H = 0.15$ demonstrated a larger peaked displacement at 10 pounds per square foot dynamic pressure.

Figures 15 and 16 show the response of the four-inch square with and without gloves. $R/H = 0.31$ and $R/H = 0.22$ are relatively the same amplitude at $f_n = 70$ cps ($Q_B = 5.0$ inches). However, at $f_n = 55$ cps

($R_B = 6.5$ inches) $R/H = 0.22$ has a definite advantage below a dynamic pressure of 30 pounds per square foot.

It is clear that the best radius for rounding the corners of a square is definitely not the best radius to be used for gloves on that same square. The ratio R/H when using gloves should be about 0.22.

Circular Cylinder

A positive advantage was derived by shrouding the sharp corners of a square. Therefore a brief look was taken at shrouding spanwise flanges located at the maximum width points ($\theta = \pm 90^\circ$) on the circular cylinder.

The recommended fix for the circular cylinder by Hite and Breckon [2] was the rotation of the beam so that the flanges would be located at the stream stagnation points. Utilization of this fix in the field was infeasible for various physical reasons.

Hite and Breckon demonstrated that the flanges when located at $\theta = \pm 90^\circ$ were responsible for the large oscillations of the circular cylinder. Without the flanges the flow separated randomly aft of the 90 degree position (present location of the flanges on the circular boom board). With the flanges installed, separation of the flow was stabilized to occur at the flanges, concentrating the energy of the lateral force at a dominant Strouhal number. The concentration of random energy in the frequency spectra results in a violent response. Therefore if the flanges can not be removed or rotated to stream stagnation points, the sharp edge effect of the flange should be eliminated.

Shrouding of the boom-board flange was expected to produce desirable responses. A one-inch radius shroud was selected, which was a ratio of shroud radius to beam diameter of 0.198 ($R/H = 0.198$). The shroud was extended laterally (into the stream flow) only far enough to cover the flange. This was a distance of only one quarter of an inch on the model, thus the cylinder retained a relatively smooth shape as is illustrated in Figure 17. The shroud was glued to the front half of the beam to provide the smoothest possible surface for the air flow.

The responses obtained are plotted on Figures 18 and 19. With a spring lever arm of three inches, the response of the possible fix exceeded the response of a square (approximately the result of a flange at 90 degrees) at a dynamic pressure of 15 pounds per square foot. The proposed fix will apparently also exceed the square's response at about

10 pounds per square foot when a spring rod length of six and one-half inches is used. A larger shroud radius relative to beam diameter might give better results. Another solution might be to blend the shroud fairing smoothly into the cylinder contour without discontinuity in surface slope.

Further expenditure of effort was not considered justified because the circular boom boards at Winter Harbor, Maine have suffered further deterioration. Replacement of the circular cylinder with rectangular-cross-section boom boards is under consideration.

5. Estimate of Unsteady Lift.

The last six runs (78 to 84) of the program were conducted in order to gain some knowledge of the lateral forcing function. Both the coefficient of lift and its spectral distribution were estimated. A sharp edged configuration was avoided for this evaluation so that a full set of data could be obtained without restriction on amplitude response. For this reason, the 5.7-inch square with one-inch corner radii ($R/H = 0.176$) was selected. The natural frequency of the beam was varied from 60 to 89 cps by adjusting the spring rod length (ℓ_B) in one-half-inch increments from six to three inches. Data were obtained at tunnel dynamic pressures up to 40 psf using intervals of two psf.

The amplitude responses (recorded on magnetic tape) were digitized to permit the use of a high-speed digital computer [7]. Utilizing the auto-correlation function, the power spectral density (P.S.D.) of the system output response was computed by the Tukey-Blackman method [1]. Sample power spectral densities of the output are shown on Figures 20 and 21. These curves are computer plotted and represent the complete set of ℓ_B values at dynamic pressures of eight and 40 psf respectively. It will be noted on Figure 20 that there are energy peaks at 24, 50, and 80 cps. These correspond to Strouhal numbers of 0.14, 0.28, and 0.45 respectively. The large energy peak at $S = 0.14$ was evident for values of q up to about 15 psf ($Re = 340,000$). The characteristics shown on Figure 21 at $q = 40$ psf ($Re = 560,000$) indicate energy peaks at $f = 41$, 80, and 123 cps which correspond to Strouhal numbers of 0.11, 0.21, and 0.32 respectively, and in general the majority of energy is at the higher Strouhal numbers. These traits were shared by the major portion of output response data when Reynolds number was above 340,000.

Computation of the power spectral density (P.S.D.) of the output from recorded data opens the door to investigation of the forcing function. $\Phi_o(f)$ the P.S.D. of the output response was normalized.

$$\int_0^{125} \Phi_o(f) df = 1.0 \quad (5)$$

The upper limit of 125 cycles per second assumes that there is no significant contribution to $\Phi_o(f)$ above that frequency. The accuracy of this assumption was checked and found to be correct for the calculations used in this report [7].

$\Phi_i(f)$ is the P.S.D. of the input forcing function, (a distributed

force acting along the length of the model, but which may be treated as a concentrated load acting at the mid-span of the model). $\Phi_i(f)$ is related to $\Phi_o(f)$ through the following relation.

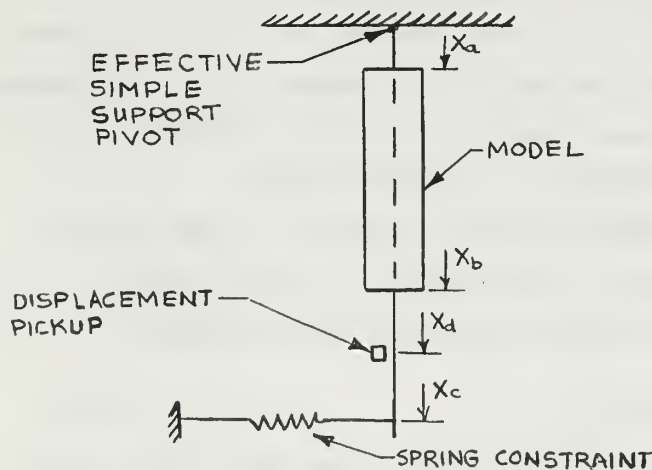
$$\Phi_i(f) = |Z(iff)|^2 \Phi_o(f) \quad (6)$$

$Z(iff)$ is the transfer function which is dependent only on the model being tested.

$$|Z(iff)|^2 = \left\{ \left[1.0 - \left(\frac{f}{f_n} \right)^2 \right]^2 + 4\beta^2 \left(\frac{f}{f_n} \right)^2 \right\} (2\pi f_n)^4 \quad (7)$$

f is the frequency in cycles per second and f_n is the natural frequency of the beam. β is the damping ratio of the beam. It was calculated by log decrement procedures on indicial-response checks. Due to the difficulty of reading the amplitudes of successive peaks with sufficient accuracy, an average β of 0.018 was used for computation of $\Phi_i(f)$. This value was obtained from eleven log decrement calculations. The damping ratio was sensitive to spring rod clamping. Various values of β (0.018 to 0.027) were used in calculating $\Phi_i(f)$ to check the effect of β . A 50 per cent increase in β resulted in less than one per cent change in $\Phi_i(f)$.

The forcing function may be found by considering the geometry of the test set up in the wind tunnel as sketched below:



Values used were:

$$\begin{aligned} X_a &= 4.0 \text{ inches} \\ X_b &= 46.0 \text{ inches} \\ X_c &= 57.0 \text{ inches} \\ X_d &= 54.0 \text{ inches} \\ I &= 35.73 \text{ slug-in}^2 \end{aligned}$$

The equation of motion for harmonic excitation may be expressed as:

$$I\ddot{\theta} + c\dot{\theta} + kX_c\theta = F \left[\frac{X_b + X_a}{2} \right] \sin \omega t \quad (8)$$

Replacing the angular coordinate by the displacement at the transducer yields:

$$Y = X_d \theta$$

$$\ddot{Y} + \frac{C}{I} \dot{Y} + \frac{K X_c}{I} Y = \frac{F X_d}{I} \left[\frac{X_b + X_a}{2} \right] \sin \omega t$$

$$\ddot{Y} + 2\beta \omega_n \dot{Y} + \omega_n^2 Y = \frac{F X_d}{I} \left[\frac{X_b + X_a}{2} \right] \sin \omega t$$

$$\text{let } \hat{M} = \frac{F X_d}{I} \left[\frac{X_b + X_a}{2} \right]$$

$$Y = \frac{\hat{M}}{|Z(i\omega)|}$$

$$\overline{\hat{M}^2} = \overline{Y^2} |Z(i\omega)|^2$$

If the mean square of the displacement is $\overline{Y^2}$, then the mean square of the applied load is:

$$\overline{\hat{M}^2} = \frac{X_d^2}{I^2} \left[\frac{X_b + X_a}{2} \right]^2 = (M.S.) (\overline{Y^2})$$

$$\text{where } (M.S.) = \int_0^{12.5} \phi_0(f) |Z(if)|^2 df$$

$$\overline{\hat{M}^2} = \frac{\overline{\hat{M}^2}}{\left[\frac{X_d}{I} \left(\frac{X_b + X_a}{2} \right) \right]^2}$$

and

$$\sqrt{\overline{C_L^2}} = \frac{\sqrt{\overline{\hat{M}^2}}}{q H (X_b - X_a)}$$

$$\text{therefore } \sqrt{\overline{C_L^2}} = \frac{[(M.S.) (\overline{Y^2})]^{1/2} (2I)}{q H X_d (X_b^2 - X_a^2)} \quad (9)$$

$\sqrt{\overline{C_L^2}}$ is the root-mean-square of the coefficient of lift.

A high-speed digital computer was utilized to calculate the root-mean-square coefficient of lift for each of the seven natural frequencies of the beam and at each dynamic pressure used. Figure 22 is the plot of the individual $\sqrt{\overline{C_L^2}}$ and Figure 23 is a plot of the average $\sqrt{\overline{C_L^2}}$. Both plots clearly indicate the occurrence of a transition at 14-pounds per square foot dynamic pressure (approximate Reynolds number of 3.3×10^5) where the flow exhibits a change to supercritical flow. All curves are essentially parallel and with only minor exceptions the beams with lower natural frequencies have larger coefficients of lift.

The consistent pattern of these plots suggests that aerodynamic forces may be induced by the motion of the models through an aeroelastic-feedback influence.

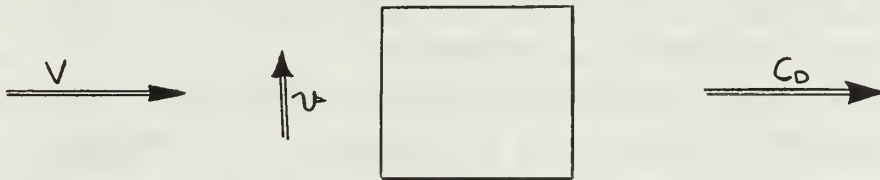
The P.S.D. of the input was also machine plotted using the digital computer to handle the transfer function type calculations. Figures 24 and 25 represent estimates for subcritical and supercritical flow and show good agreement for all values of model resonant frequency with respect to the occurrence of energy peaks.

The peaks of the power spectral density curves of the exciting force occurred at a constant Strouhal number. For dynamic pressure up to and including 12 pounds per square foot ($Re = 3.1 \times 10^5$) the vortex shedding occurred at a Strouhal frequency of 0.140. At and above 16 pounds per square foot ($Re = 3.5 \times 10^5$) the Strouhal frequency was 0.32. At 14 pounds per square foot ($Re = 3.3 \times 10^5$) two peaks were present, one at a Strouhal number of 0.14 and the other at 0.32. The beams with natural frequencies below 75 cycles per second (70, 65, and 60 cycles per second) responded at a Strouhal number of 0.32.

The 14 pounds per square foot reading was obviously in the flow transition region. Supercritical flow was experienced at a dynamic pressure of 16 pounds per square foot ($Re = 3.5 \times 10^5$). Dr. Fung found that the critical Reynolds number for his circular cylinder was $Re = 3.0 \times 10^5$ [6].

The aeroelastic-feedback term was further investigated by considering $\sqrt{\overline{C_L}}$ results of Figure 22 at dynamic pressures of 10 and 30 psf which correspond to Reynolds numbers of 280,000 and 480,000 respectively. The fluctuating lift values are cross plotted on Figure 26 as a function of the normalized lateral response. It will be noted that both flow conditions have approximately linear dependence upon motion, and the subcritical flow appears to extrapolate to a value of $\sqrt{\overline{C_L}} = 0.35$ for a rigid model while the corresponding supercritical flow value is about 0.075. A graphical procedure has been used on Figure 26 to obtain an aeroelastic gain correction for the subcritical flow case, normalized such that the gain value is zero for the rigid case. The large influence of motion on fluctuating loads is quite surprising, especially when one notes that lateral displacement (R.M.S.) on the order of one hair thickness more than doubles the value of fluctuating load.

A simple model may be conjectured to describe the build-up of an aeroelastic feedback term. The model assumes that fluctuating lift is developed due to the instantaneous response of a rotating drag vector, with the rotation being caused by the motion-induced angle of attack changes. Consider a bluff body moving laterally in rectilinear flow as shown in the sketch below:



If $y = y_0 \sin \omega t$,

then $\frac{dy}{dt} = \dot{y} = y_0 \sin \omega t$

hence $v_{MAX} = 2\pi f y_0$

and $\overline{v^2} = 2\pi^2 f^2 \overline{y^2}$

Therefore the mean-induced angle is given by:

$$\overline{\alpha^2} = \frac{\overline{v^2}}{\overline{V^2}} = 2\pi^2 \frac{f^2}{V^2} \overline{y^2}$$

But if there exists a dominant Strouhal number that defines the frequency, then $f = VS/H$.

Hence $\overline{\alpha^2} = 2\pi^2 S^2 \left(\frac{\overline{y^2}}{H^2} \right)$

If we assume that $C_L(t) = \alpha(t) C_{D\text{STEADY}}$

then $\sqrt{\overline{C_L^2}} = \sqrt{2} \pi S \frac{\sqrt{\overline{y^2}}}{H} C_{D\text{STEADY}} \quad (10)$

and $\frac{d\sqrt{\overline{C_L^2}}}{d\left(\frac{\sqrt{\overline{y^2}}}{H}\right)} = \sqrt{2} \pi S C_{D\text{STEADY}} \quad (11)$

For the square cylinder with rounded corners under the condition of subcritical flow, we may assume $S = 0.14$ and $C_D = 1.0$. Hence an estimate

of the aeroelastic effect would be

$$\frac{d\sqrt{\overline{C_L^2}}}{d\left(\sqrt{\frac{\overline{y^2}}{H}}\right)} = \sqrt{2} \pi (0.14)(1.0) = 6.2 \times 10^{-1}$$

The actual slope estimated from Figure 26 is 5×10^3 , a value approximately four orders of magnitude greater than that predicted by the simple model. The large discrepancy would indicate that either the experimental procedures and estimates presented here are suspect or that the simple model is completely inadequate.

The existence of fluctuating loads on a rigid model seems reasonable since the unsteady pressure exist in separated flow, independent of motion. The dependence of these pressures and their instantaneous integrated value (net fluctuating force) upon motion is not clear, and further study certainly seems worthwhile.

6. Summary.

The large responses of the square-cross-section boom boards were sharply reduced by two different modifications to the beams. Rounding the corners on solid boom boards at the time of construction appeared to be a desirable solution. A ratio of corner radius to frontal width of 0.263 provides a response that is near the level of a circular cylinder for all wind velocities (up to 171 miles per hour) that may be encountered.

A retrofit modification was tested for use on boom boards that are presently installed as part of the Wullenwebber Antenna system. This fix consisted of shaped shrouds which would be attached over the corners of the boom boards. The desirable ratio of shroud radius to the length of the side of the square should be about 0.22 to 0.25.

A shroud for the flange on the circular cylinder was tested, but no appreciable improvement was noted. A different size and or shape of shroud might produce a marked reduction in amplitude response, but further studies in this direction were not made.

Tunnel tests demonstrated a correlation between models of different H/D ratios (ratio of frontal width to depth of model) in the Reynolds number supercritical flow region. The first order components of the amplitude responses were found to be inversely proportional to the H/D ratios (when holding frontal width constant), thereby showing that the fluctuating pressures developed on the lateral faces are not too sensitive to the length of that face. The dominant factor appears to be corner radius ratio.

The use of precision instrumentation, magnetic recording of data, and data processing by analog and digital computers permitted investigation of the forcing function's power spectral density and lateral root-mean-square coefficient of lift. The coefficients of lift were estimated for the square with rounded corners and were compared with previously published information on circular cylinders. The dependence of unsteady lift upon motion strongly suggests the influence of an aeroelastic feedback term. Further investigations should be conducted in this area with different size models to confirm and/or isolate the aeroelastic feedback component.

BIBLIOGRAPHY

1. Blackman, R. B. and J. W. Tukey. The Measurement of Power Spectra. Dover, 1959.
2. Breckon, R. L. and P. R. Hite. Wullenwebber Antenna Vibration Study, Thesis U. S. N. Postgraduate School, 1965.
3. Delaney, N. K. and N. E. Sorensen. Low-Speed Drag of Cylinders of Various Shapes, NACA Report TN 3038. November 1953.
4. Fung, Y. C. An Introduction to the Theory of Elasticity. John Wiley and Sons, 1955.
5. Fung, Y. C. Fluctuating Lift and Drag Acting on a Cylinder in a Flow at Supercritical Reynolds Numbers. Technical Report GM - TR - 0165-00343. 7 May 1958.
6. Fung, Y. C. The Analysis of Wind-Induced Oscillations of Large and Tall-Cylindrical Structures. Technical Report STL/TR-60-000-009134. June 1960.
7. Jesberg, R. J. Data Handling Procedures in Support of Aeroelastic Problems in an Antenna Vibration Project. Thesis U. S. N. Postgraduate School, to be published, May 1966.
8. Keefe, R. T. An Investigation of the Fluctuating Forces Acting on a Stationary Circular Cylinder in a Subsonic Stream and of Associated Sound Field. Univ. of Toronto, UTIA Report 76. 1961
9. Roshko, A. Experiments on the Flow Past a Circular Cylinder at Very High Reynolds Number. Journal of Fluid Mechanics, v. 10, part 3, 1961:345-356.

Table I

RUN SCHEDULE

Date	Run	Configuration	q(PSF)	ρ_B	Data
10-22	20	Circ Cyl	20	8.88	F,A,D,T
10-26	21	Circ Cyl	5-10	8.88	F,A,D
	22	Circ Cyl	5-40	8.88	F,A,D,T
	23	Circ Cyl	5-40	6.00	
	24	Circ Cyl	5-40	3.00	
10-27	25	Sqr Cyl	5-20	3.00	
	26	Sqr Cyl	5-12	5.00	
	27	Sqr Cyl	3- 8	6.50	
10-29	28	5.7 Sqr & .50 RC	3-10	6.50	
	29		5-15	5.00	
	30		5-30	3.00	
	31	Front-5.7 Sqr & .50 RC Rear-Rect Cyl	5-25	3.00	
10-30	32		3-10	6.50	
	33	Rect Cyl	3- 8	6.50	
	34		5-15	5.00	
	35		5-20	3.00	
	36	Front-Rect Cyl Rear-5.7 Sqr & .50 RC	5-15	3.00	
11-1	37	Sqr Cyl & 1.00 RC	5-40	3.00	
	38			5.00	
	39			6.50	
	40	5.7 Sqr & 1.50 RC		6.50	
	41		5-40	5.00	
	42			3.00	
11-2	43	5.7 Sqr & 2.00 RC		3.00	
	44			6.50	
	45			5.00	
1-24	46	5.7 Sqr & 2.00 RC	5-40	5.00	D
	47	5.7 Sqr & 1.25 Glove		3.00	D
	48			5.00	D
	49			6.50	D

Table 41

RUN SCHEDULE (CONT'D.)

Date	Run	Configuration	q (PSF)	ℓ_B	Data
2-11	50	5.7 Sqr & 1.25 Glove	5.40	6.50	A,D
↓	51	↓	↓	3.00	A,D
2-14	52	5.7 Sqr & 1.25 Glove	↓	3.00	F,A,D,T
↓	53	↓	↓	5.00	↓
↓	54	↓	↓	6.50	↓
↓	55	5.7 Sqr & .875 Glove	↓	6.50	↓
↓	56	↓	↓	5.00	↓
↓	57	↓	↓	3.00	↓
2-15	58	5.7 Sqr	5-20	3.00	↓
↓	59	5.7 Sqr	5-15	5.00	↓
↓	60	4.00 Sqr	5-12	5.00	↓
↓	61	4.00 Sqr	3- 8	6.50	↓
↓	62	4.00 Sqr	5-20	3.00	↓
2-18	63	4.00 Sqr & .875	5-40	3.00	F,A,D,T
↓	64	↓	↓	5.00	↓
↓	65	↓	↓	6.50	↓
↓	66	4.00 Sqr 1.25 Glove	↓	5.00	↓
↓	67	↓	↓	3.00	↓
↓	68	↓	↓	6.50	↓
↓	69	6.00 x 4.00 Rect	3- 8	6.50	↓
↓	70	↓	3-15	5.00	↓
↓	71	↓	5-25	3.00	↓
2-21	72	6.00 x 3.00 Rect	5.25	3.00	↓
↓	73	↓	5-20	5.00	↓
↓	74	↓	3-10	6.50	↓
↓	75	Circ Cyl 1.00 R over flange	5-40	6.50	↓
↓	76	↓	5-40	5.00	↓
↓	77	↓	5-35	3.00	↓
2-22	78	5.7 Sqr & 1.00 RC	5.40	3.00	F,D,T
↓	79	↓	↓	3.50	↓

Table L

RUN SCHEDULE (CONT'D.)

Date	Run	Configuration	q(PSF)	l_B	Data
2-25	80	5.7 Sqr & 1.00 RC	5-40	4.00	F,D,T
↓	81	↓	↓	4.50	↓
	82			5.00	
	83			5.50	
↓	84	↓	↓	6.00	↓

RC - Radius of Corners

Circ - Circular

Cyl - Cylinder

Sqr - Square

Rect - Rectangular

l_B - Length of Spring Rod

Data Code:

F - Frequency Response Measured (Tunnel-off)

A - Acceleration Readings Recorded

D - Displacement Readings Recorded

T - Data Recorded on Magnetic Tape

All lengths in inches

Table II
Scaling Study Calculations
Square Cross Section

A. Reference Data

Case	Run	H (in.)	l_B (in.)	f_n (cps)	q (psf)	S_n	$\sqrt{y^2}$ (10^{-3} in.)	$\sqrt{y^2}/H$ ($\times 10^{-3}$)
a	58	5.7	3.0	89	20.0	0.32	6.57	1.15
b	59	5.7	5.0	70	13.0	0.32	11.15	1.96
c	62	4.0	3.0	89	10.0	0.32	1.37	0.34
d	60	4.0	5.0	70	6.5	0.32	2.75	0.69
e	61	4.0	6.5	55	4.0	0.32	3.20	0.80

B. Comparison

Cases	$\frac{\sqrt{y_1^2}}{\sqrt{y_2^2}}$ ①	$\left[\frac{q_1 H_1}{q_2 H_2} \right] \left[\frac{f_{n_2}}{f_{n_1}} \right]^2$ ②	$\frac{\sqrt{C_{L_1}^2}}{\sqrt{C_{L_2}^2}}$ ①/②
(d):(c)	2.00	1.05	1.90
(e):(c)	2.34	1.05	2.35
(a):(c)	4.80	2.83	1.69
(b):(c)	8.15	2.99	2.72

Table III
H/D Calculations

f_n (cps)	q (psf)	H/D	$\sqrt{y^2}$ (10^{-3} inch)	Amp* Ratio	Inverse H/D Ratio
89	25	2.0	4.79	.70	.75
		1.5	6.85	1.00	1.00
		1.0			1.50
	20	2.0	3.21	.67	.75
		1.5	4.79	1.00	1.00
		1.0	6.57	1.65	1.50
	15	2.0	1.97	.73	.75
		1.5	2.70	1.00	1.00
		1.0	3.90	1.44	1.50
70	15	2.0	9.43	.67	.75
		1.5	14.0	1.00	1.00
		1.0	20.2	1.44	1.50
	10	2.0	4.79	.75	.75
		1.5	6.4 (EST)	1.00	1.00
		1.0	8.6 (EST)	1.35	1.50
	5	2.0	2.03	.77	.75
		1.5	2.63	1.00	1.00
		1.0	3.60	1.37	1.50

* Amplitude ratio is defined relative to the amplitude of the bluff body with H/D = 1.50.

FIGURE 1
ANTENNA INSTALLATION
GENERAL LAYOUT

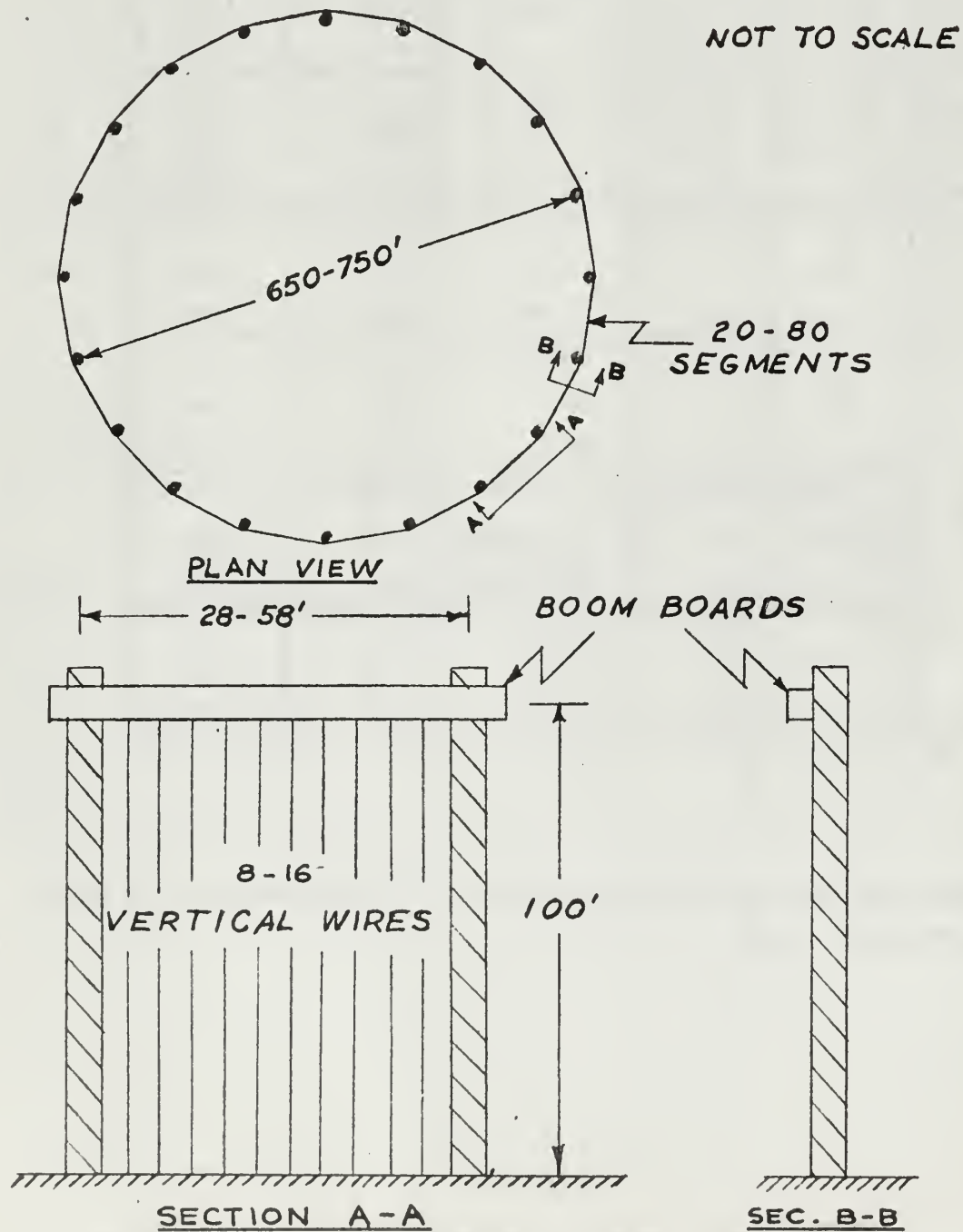


FIGURE 2
TYPICAL BOOM BOARD
CROSS SECTIONS

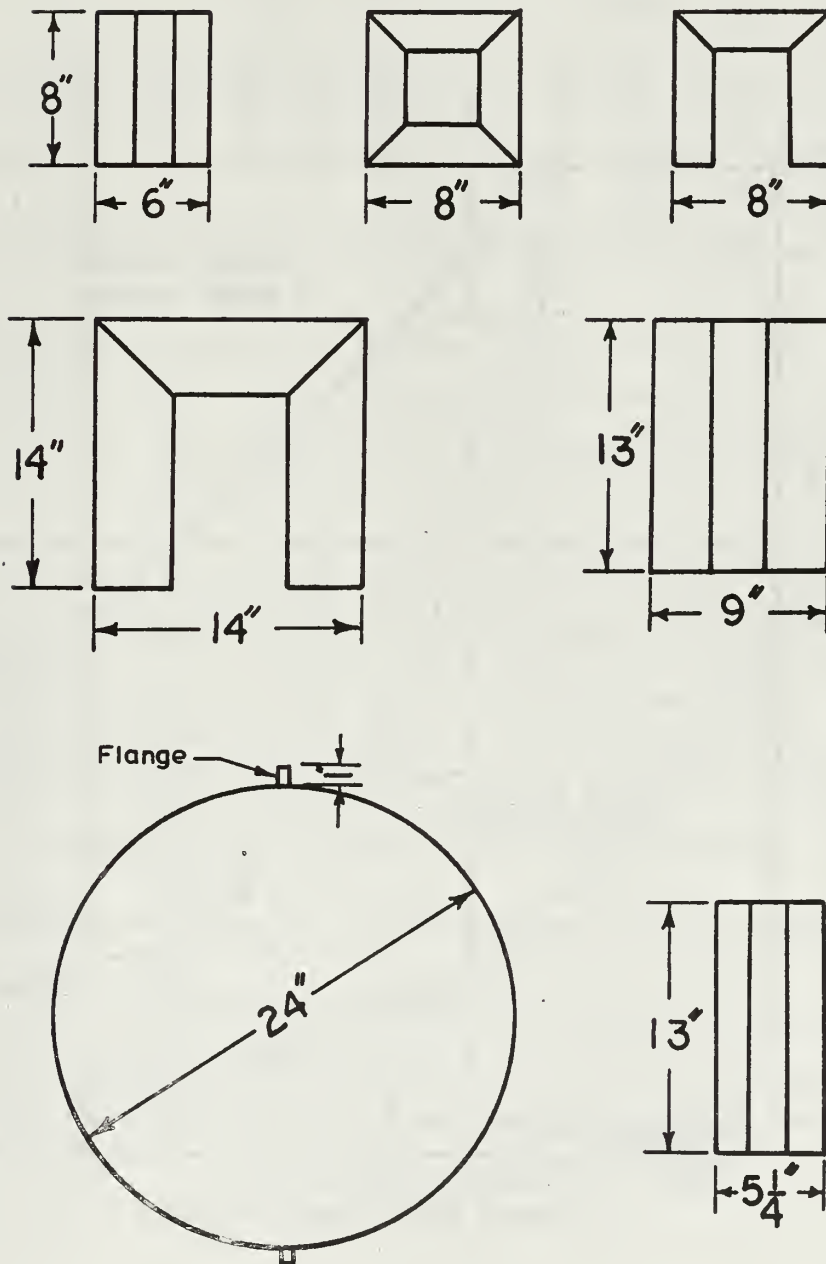


FIGURE 3
SPRING BAR CALIBRATION

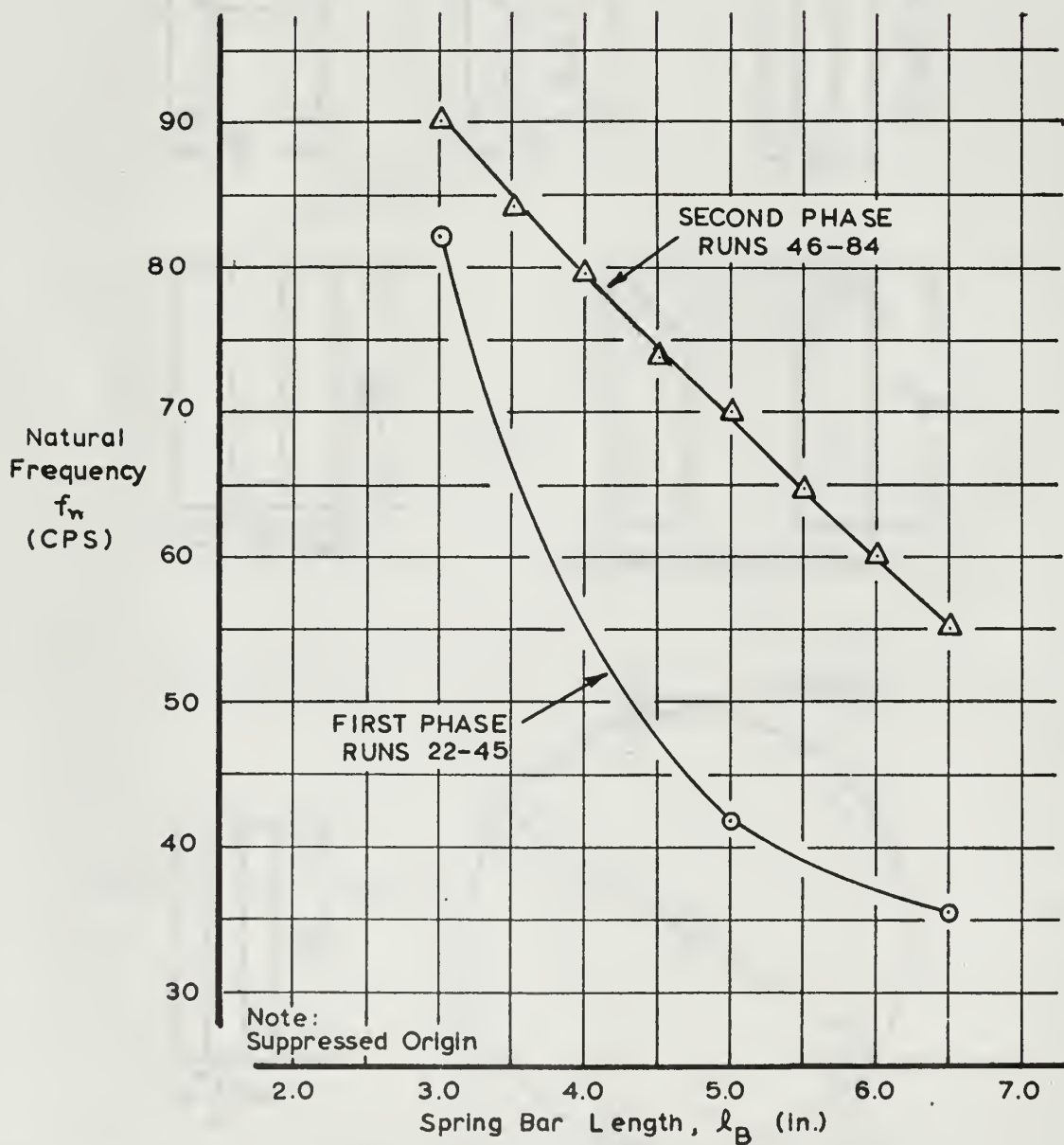


FIGURE 4
DYNAMIC RESPONSE, SQUARE CYLINDER

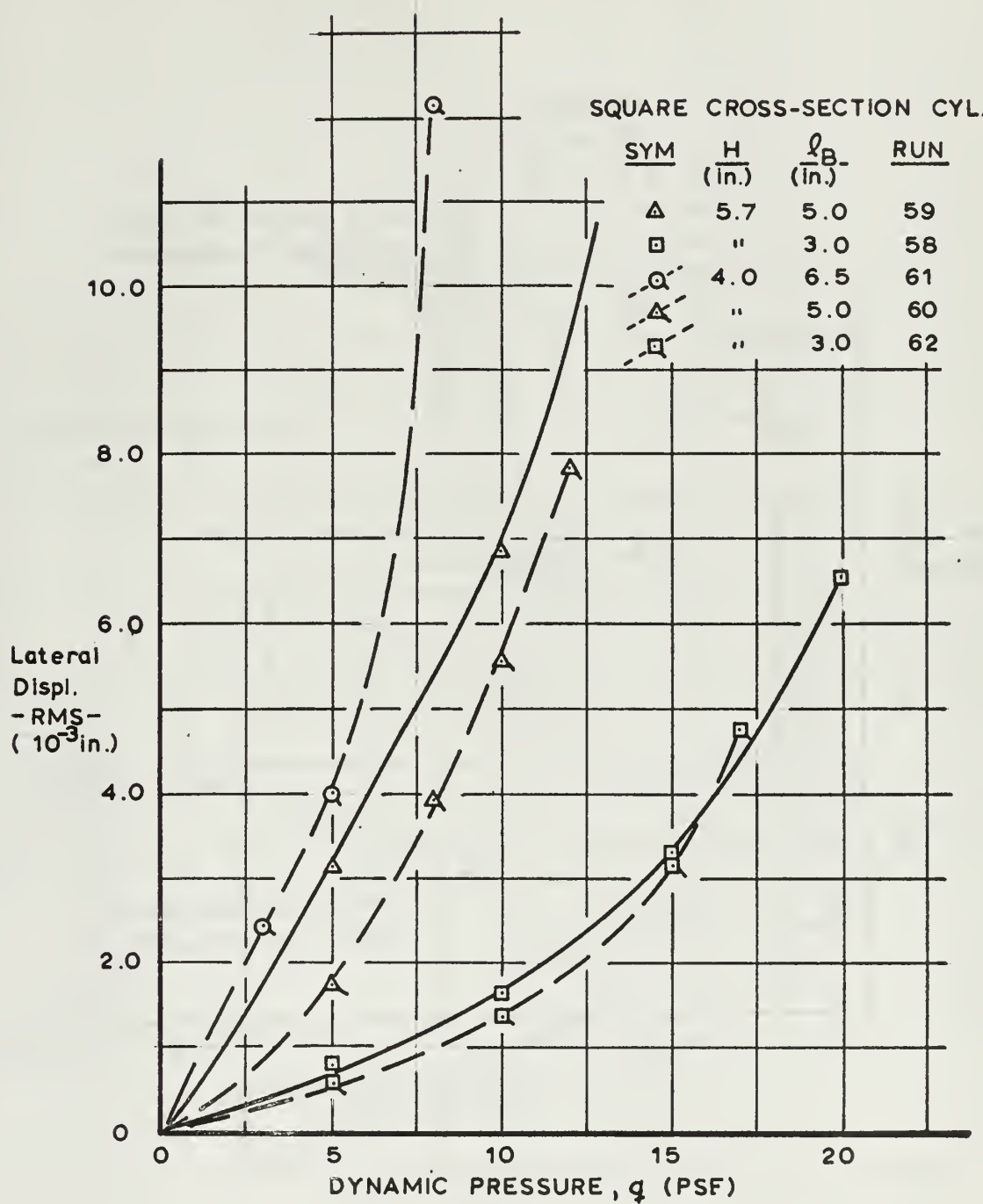


FIGURE 5
EFFECTS OF MOTION ON LIFT,
SQUARE CYLINDER

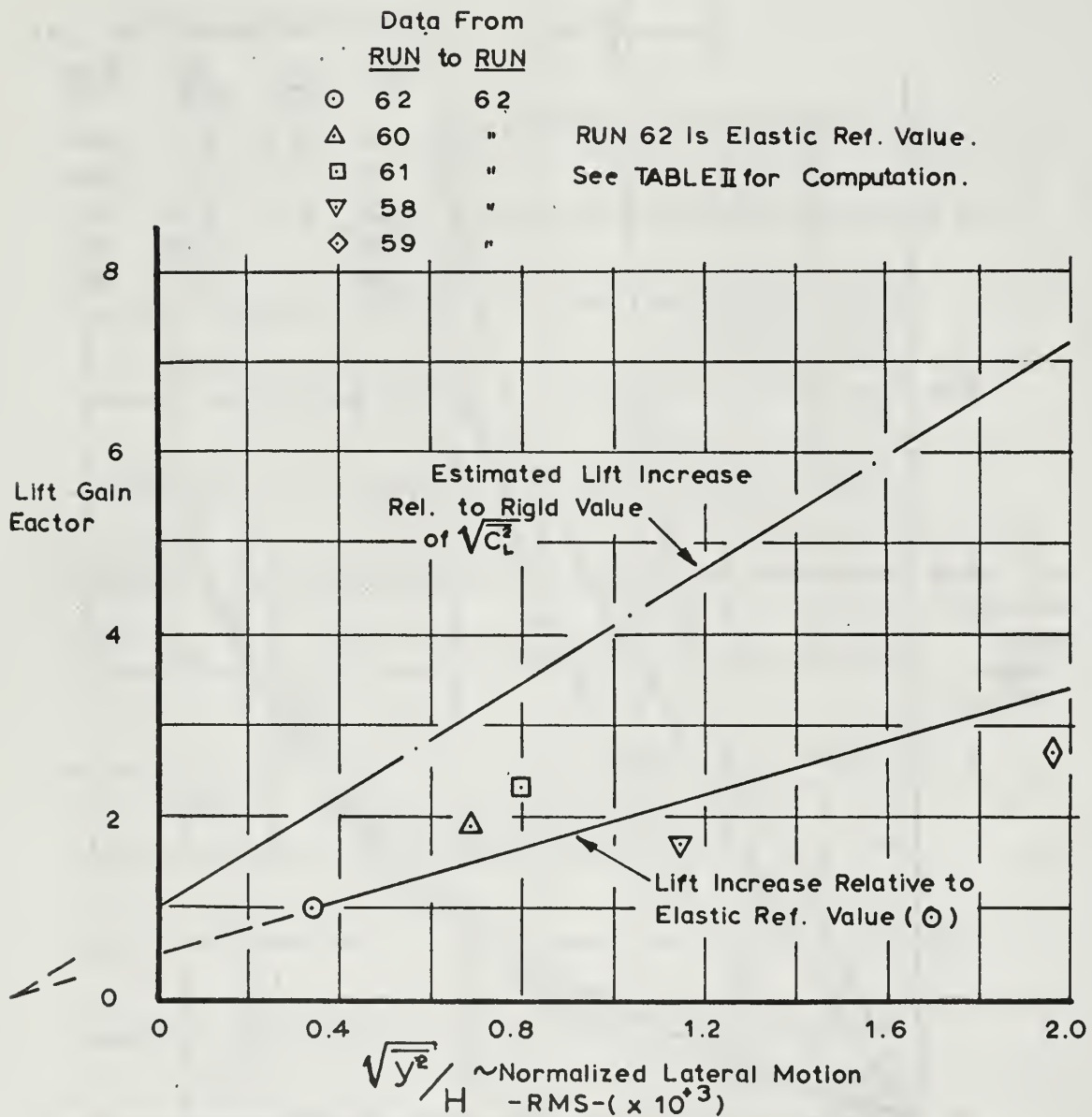


FIGURE 6
EFFECTS OF H/D RATIO, $l_B=3$ INCHES

RECTANGULAR CROSS SECTN. CYLS., $l_B=3.0$ in.

<u>SYM</u>	<u>H/D</u>	<u>RUN</u>
Δ	1.0	58
\square	1.5	71
\circ	2.0	72

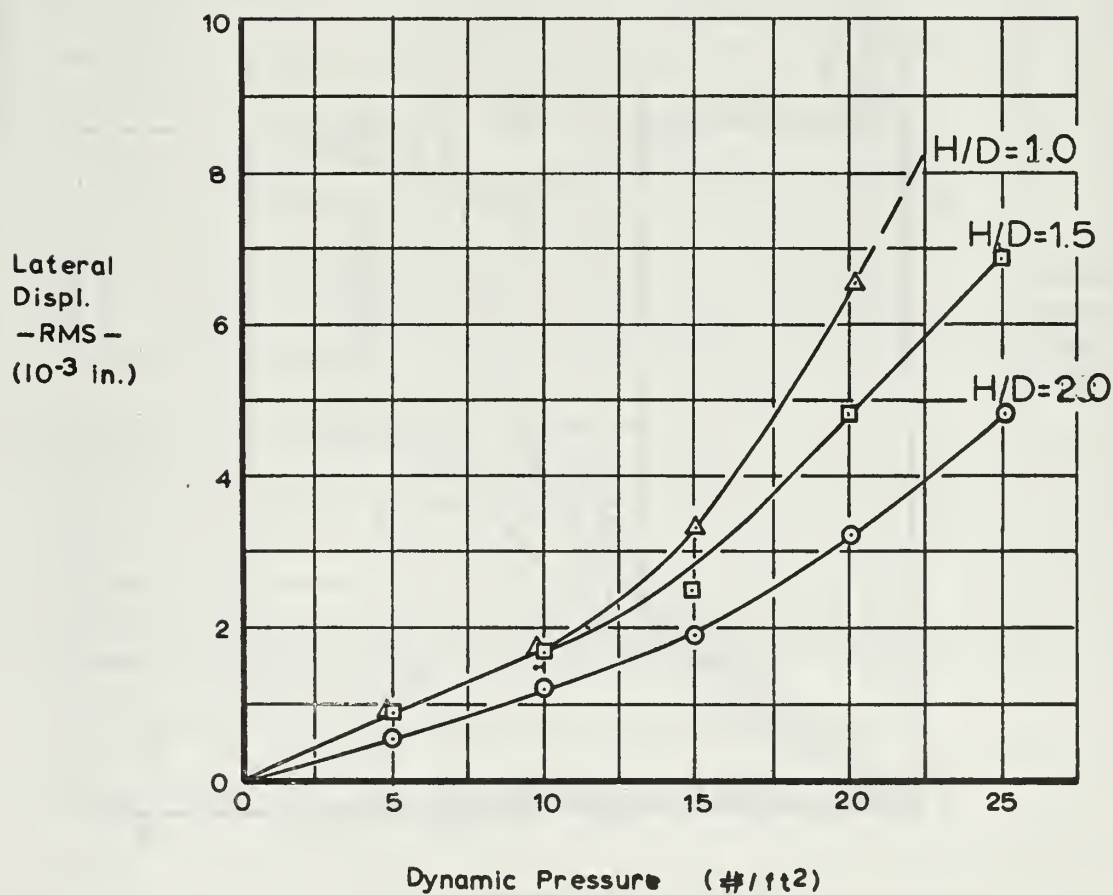
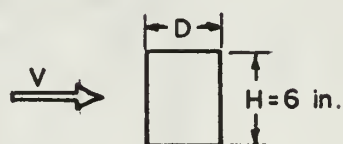


FIGURE 7
EFFECTS OF H/D RATIO, $l_B = 5$ INCHES

RECTANGULAR CROSS-SECT. CYLS., $l_B = 5.0$ in.

SYM	H/D	RUN
△	1.0	59
□	1.5	70
○	2.0	73

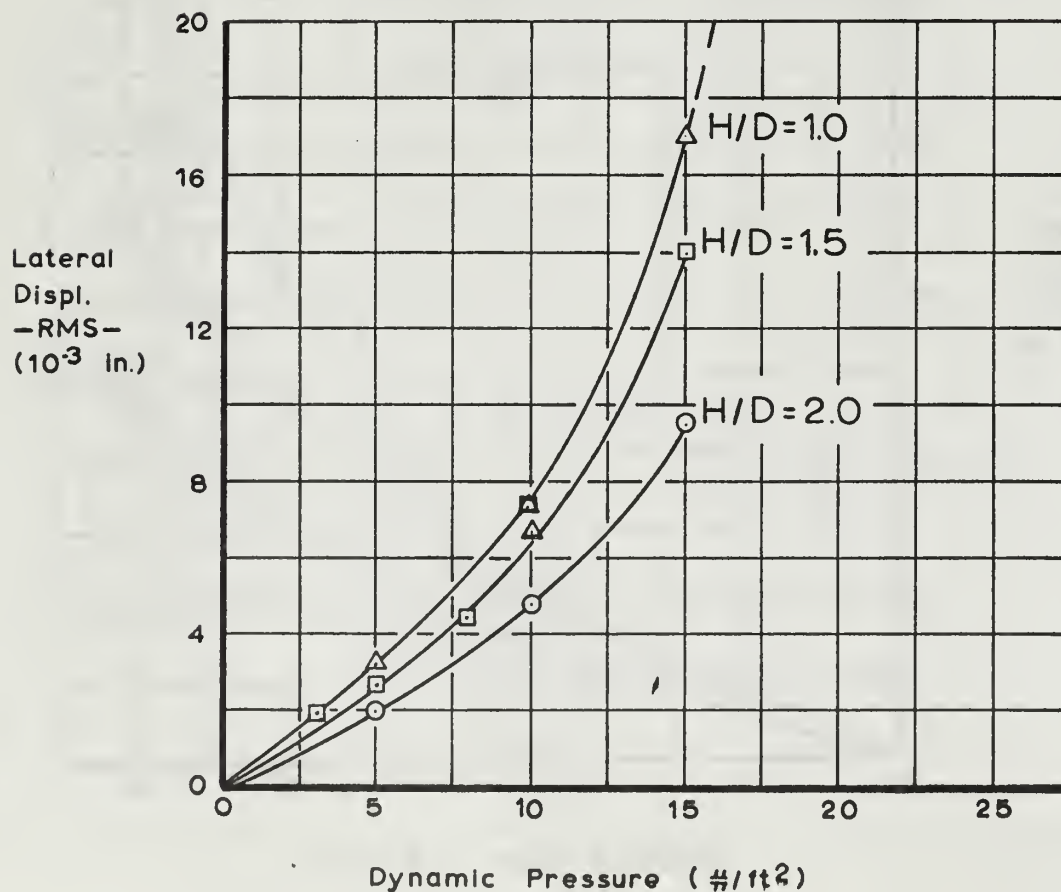
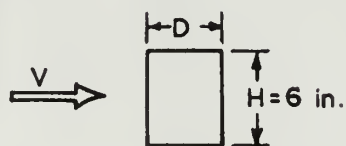


FIGURE 8
BLUFF BODY DRAG SUMMARY

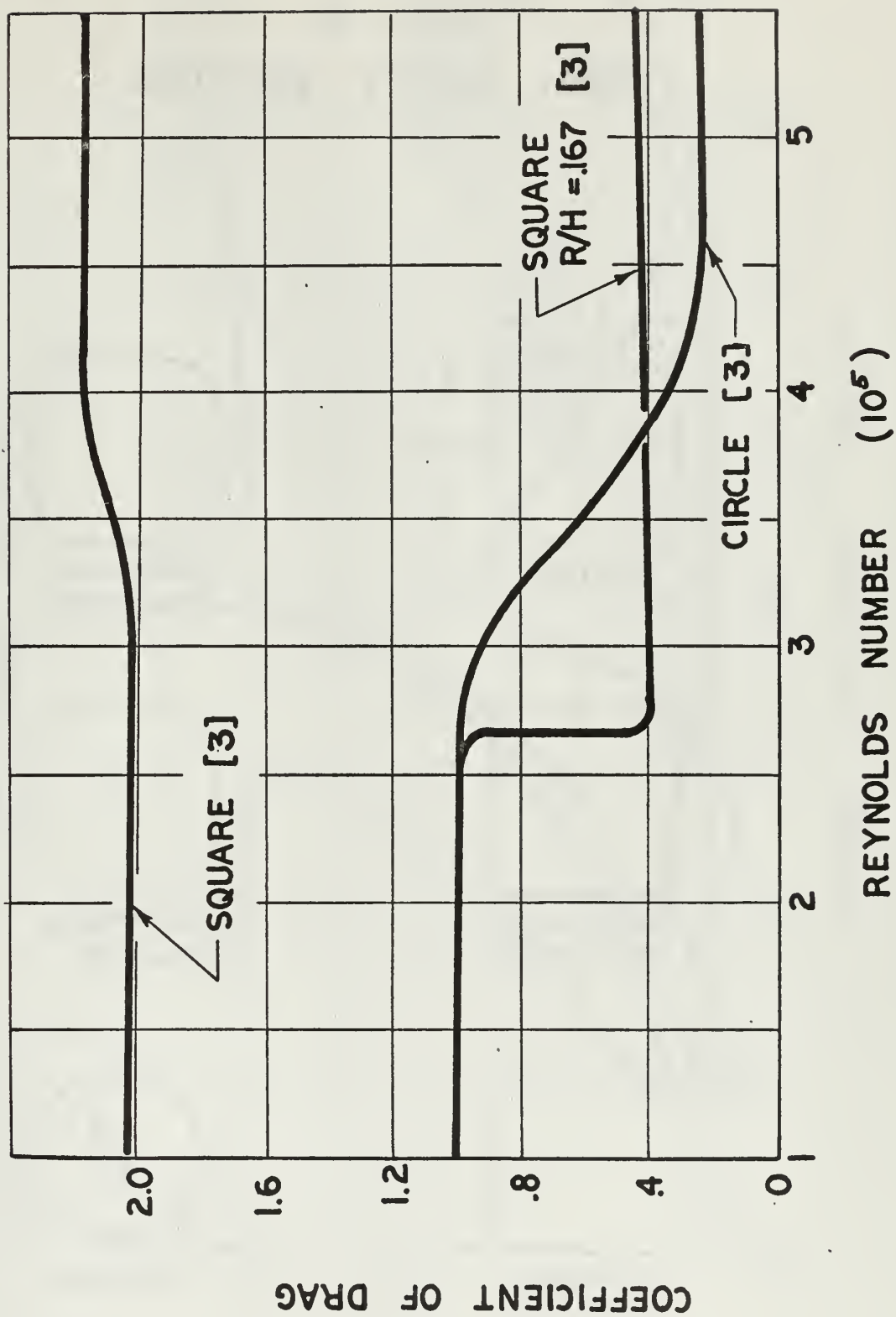
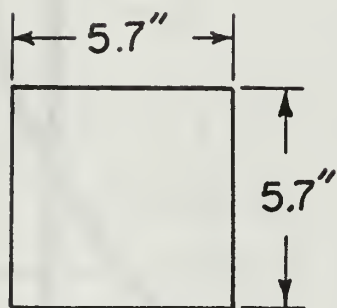


FIGURE 9
MODEL CROSS SECTIONS



Square



1.5" Radius
 $R/H=0.263$



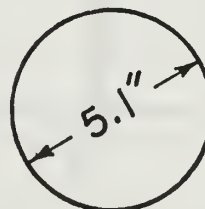
0.5" Radius
 $R/H=0.0877$



2.0" Radius
 $R/H=0.351$



1.0" Radius
 $R/H=0.176$



Cylinder

FIGURE 10
EFFECTS OF CORNER RADII
ON DYNAMIC RESPONSE

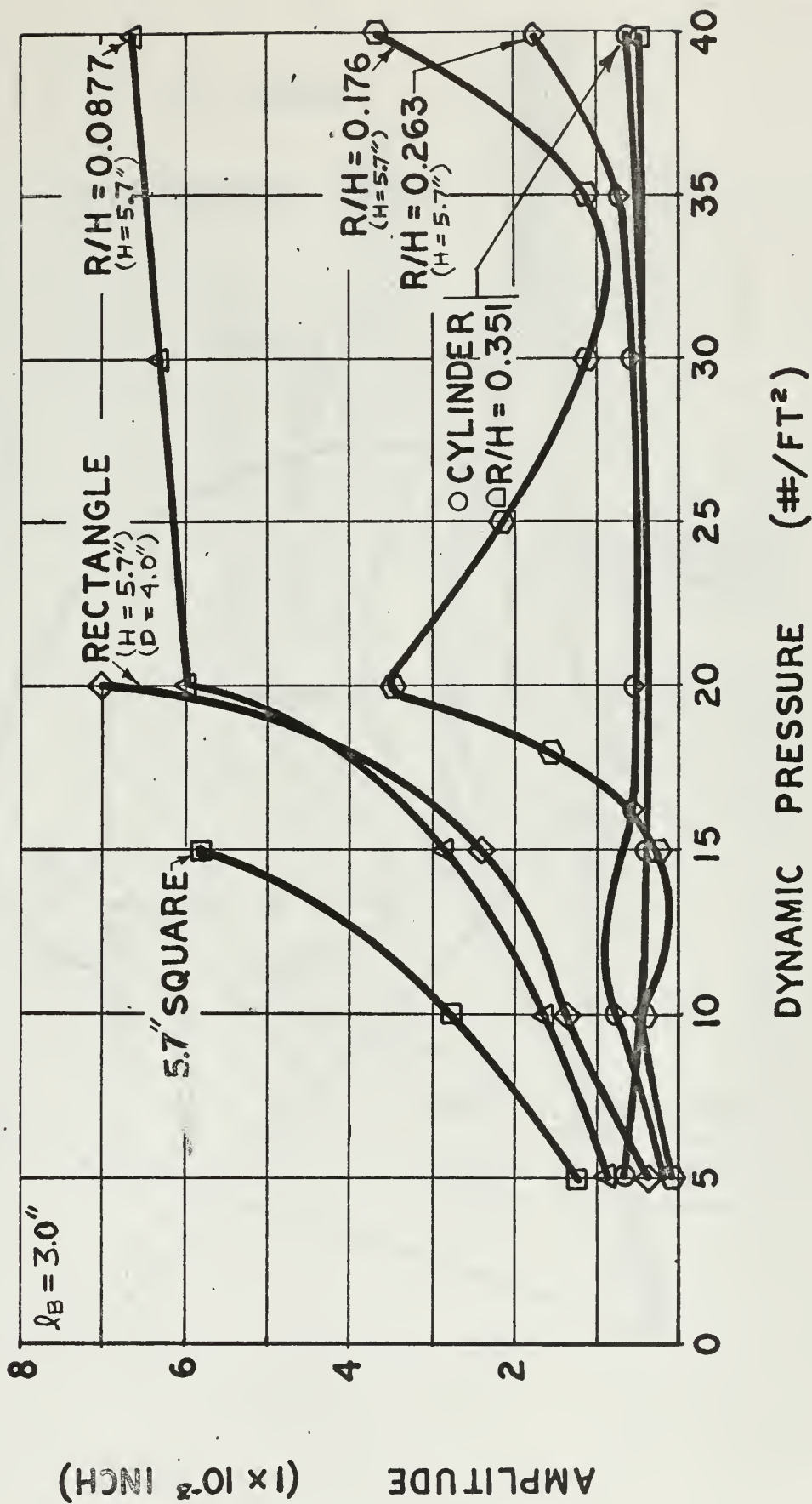


FIGURE 11

GLOVE GEOMETRY

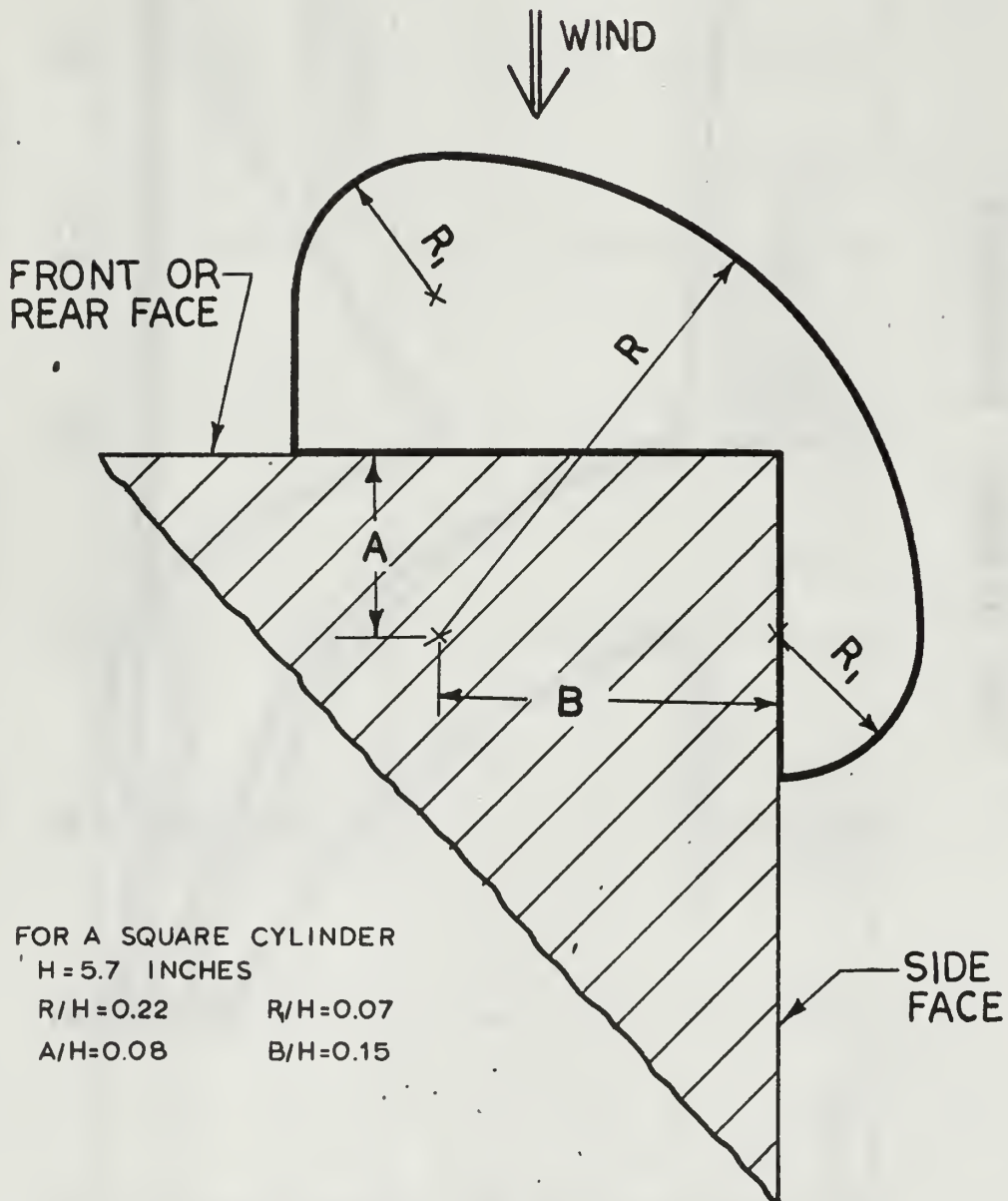


FIGURE 12
EFFECTS OF GLOVES
 $\ell_B = 6.5$ INCHES

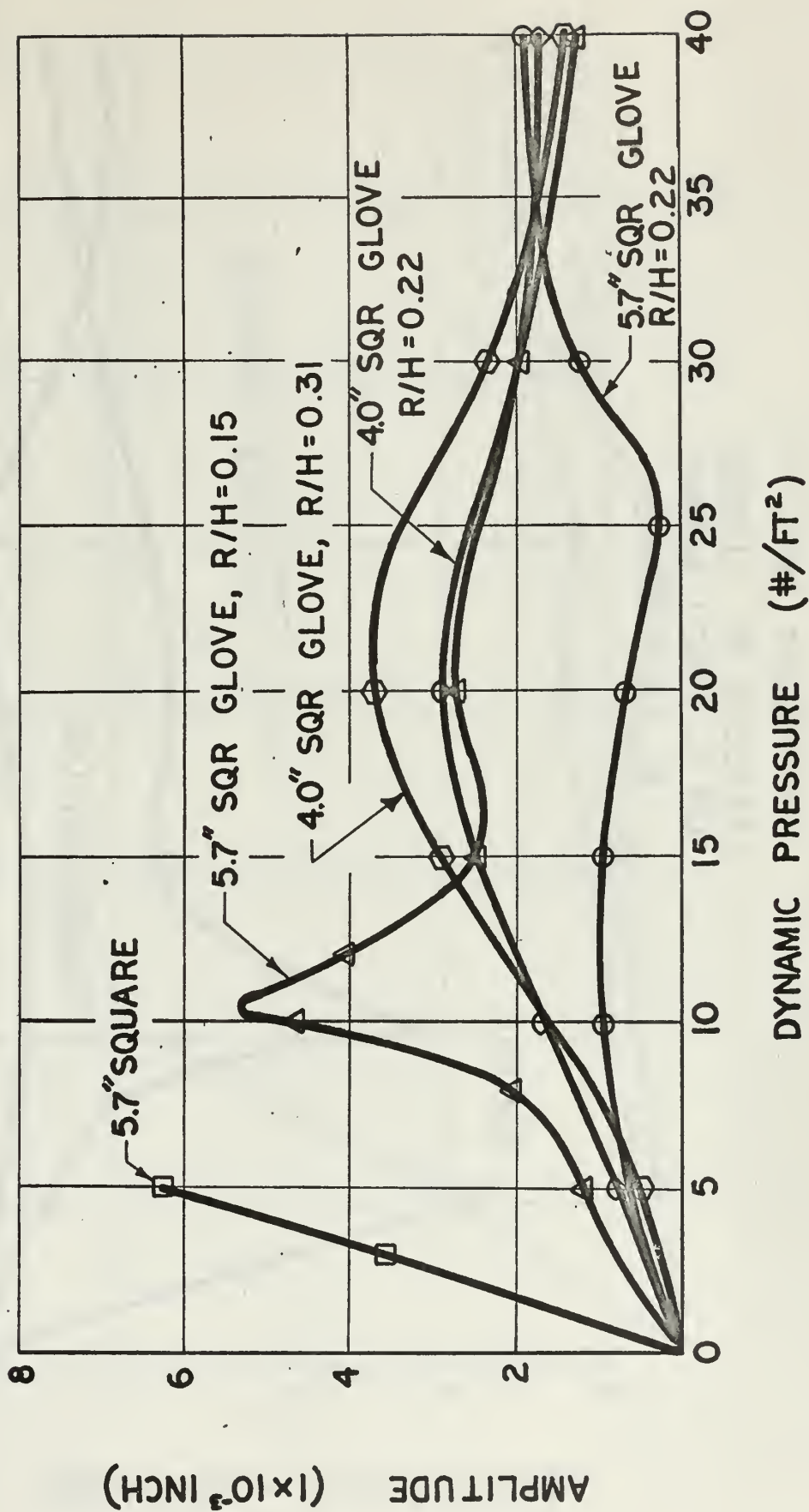


FIGURE 13
EFFECTS OF GLOVES
ON 5.7 - INCH SQUARE
 $\lambda_B = 6.5$ INCHES

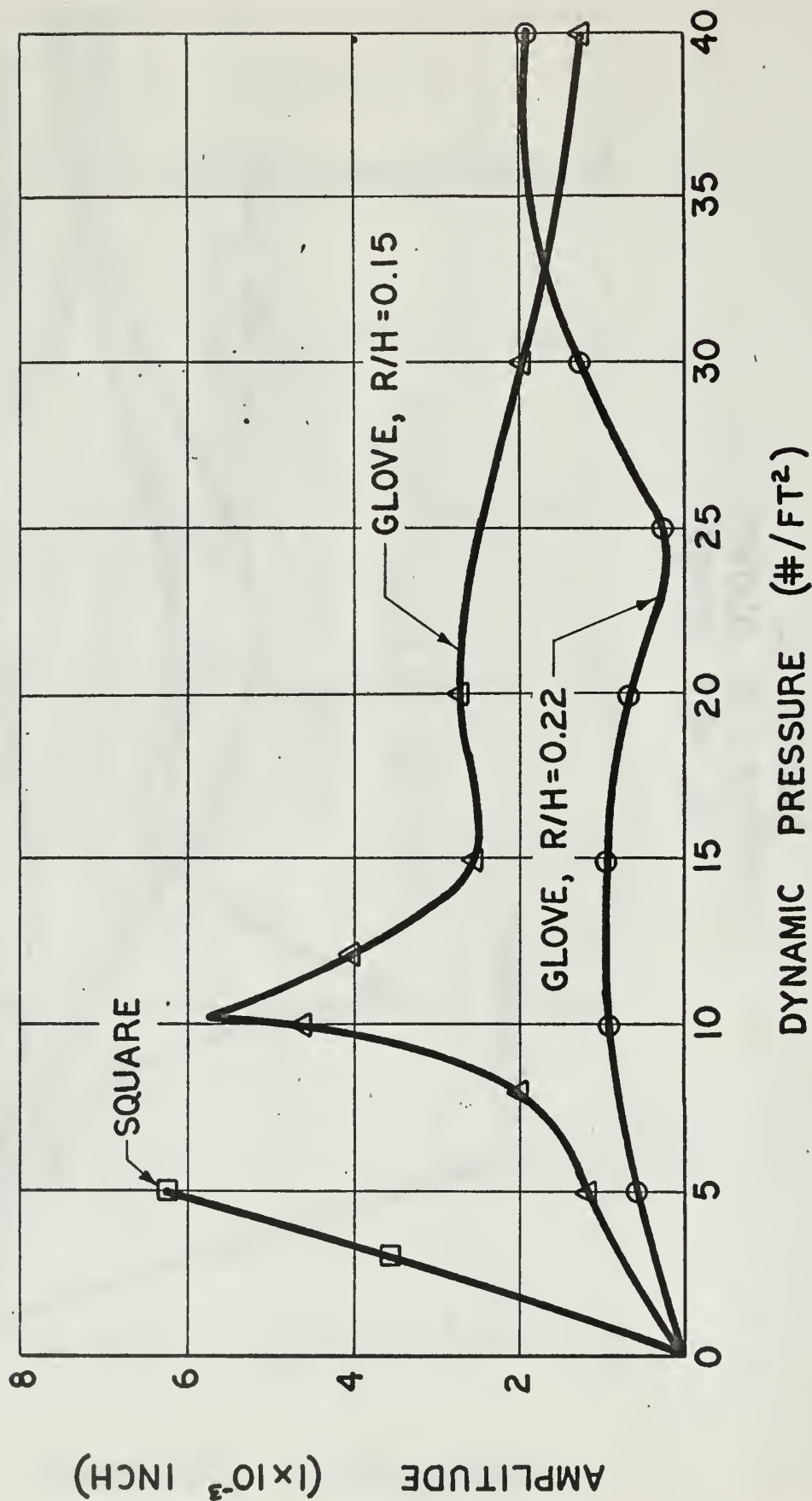


FIGURE 14
EFFECTS OF GLOVE
ON 5.7-INCH SQUARE
 $\rho_B = 5.0$ INCHES

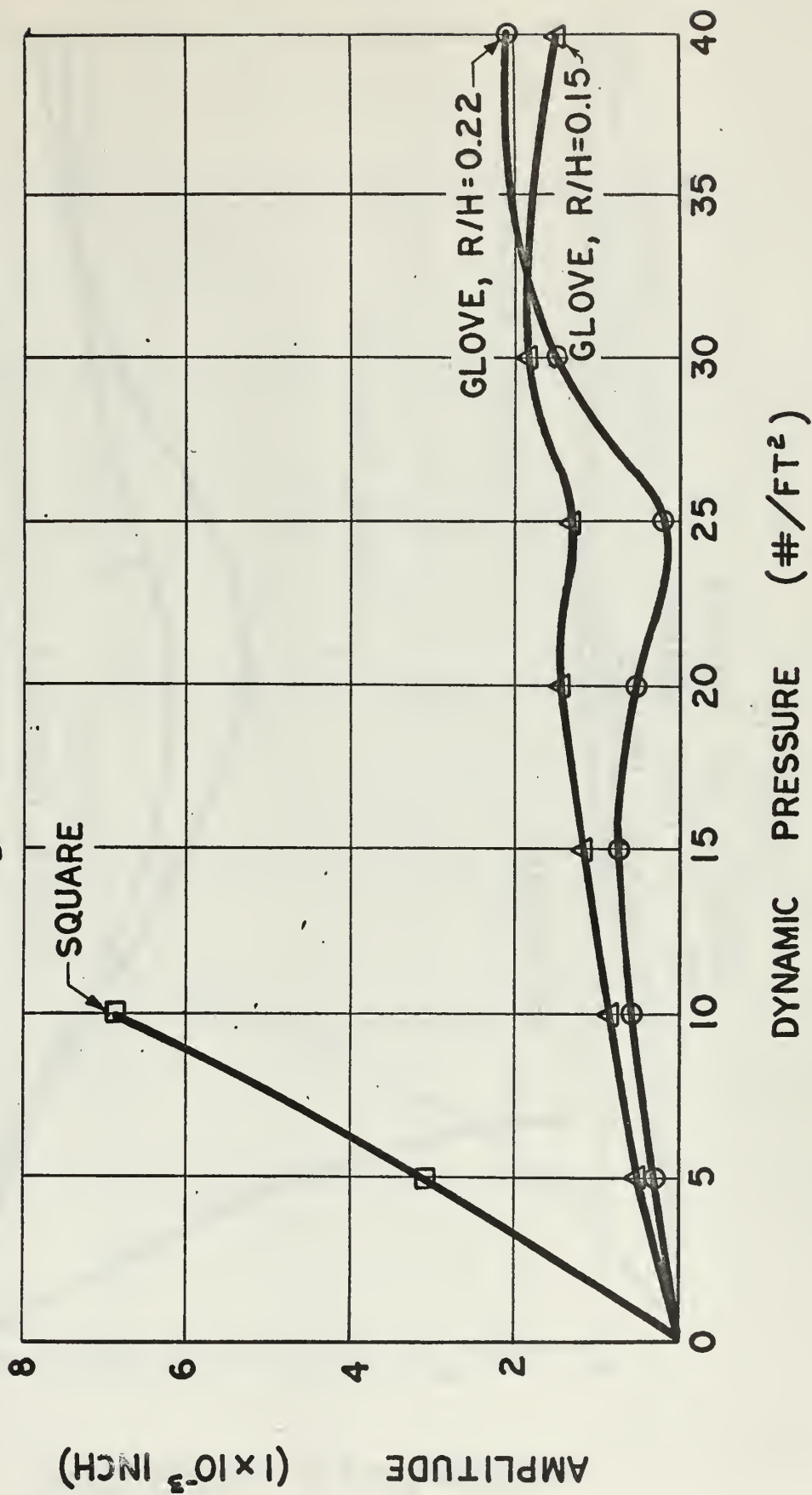


FIGURE 15
EFFECTS OF GLOVES
ON 4.0 -INCH SQUARE
 $\lambda_B = 6.5$ INCHES

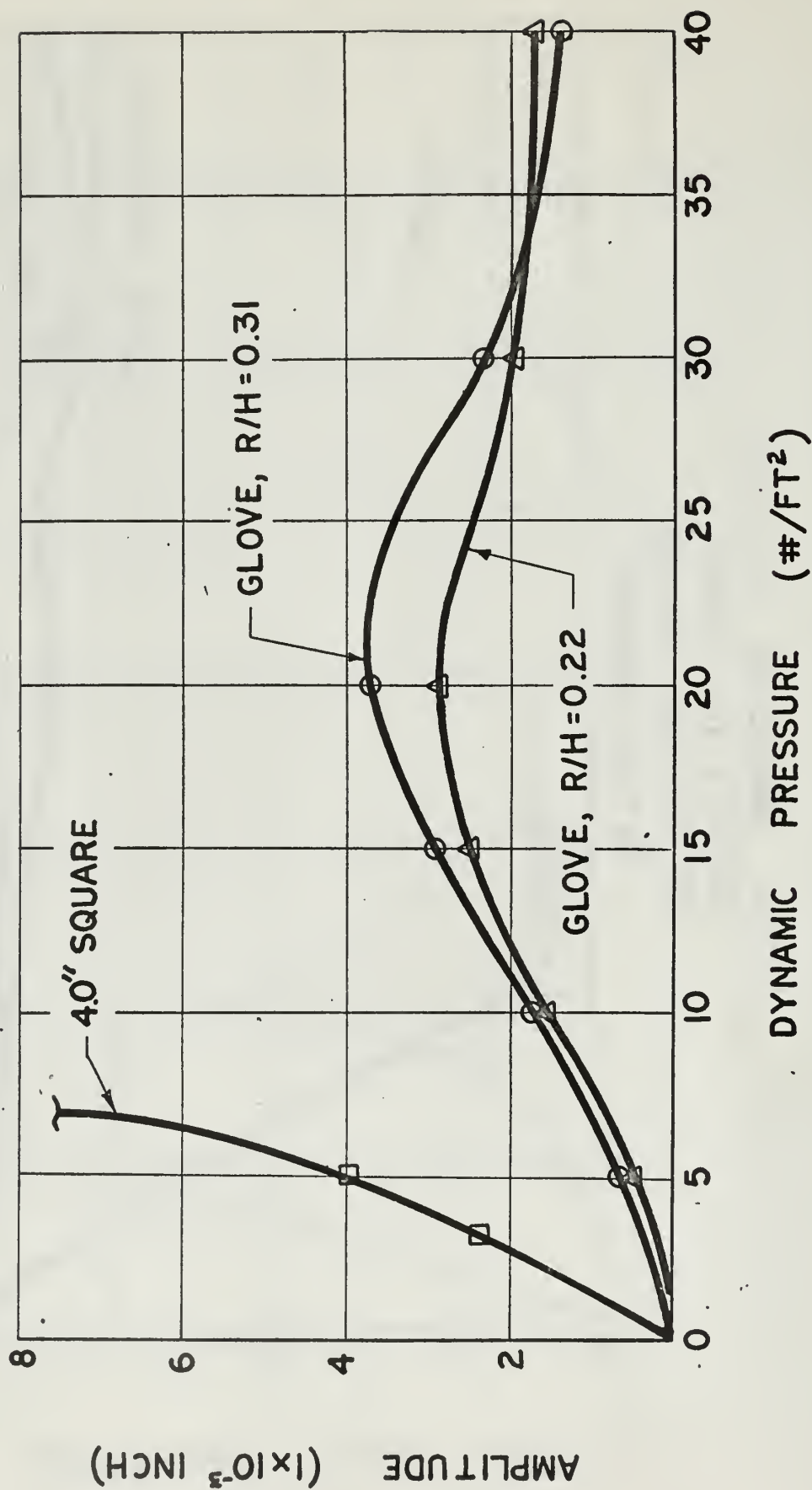


FIGURE 16
EFFECTS OF GLOVE
ON 4.0-INCH SQUARE
 $\rho_B = 5.0$ INCHES

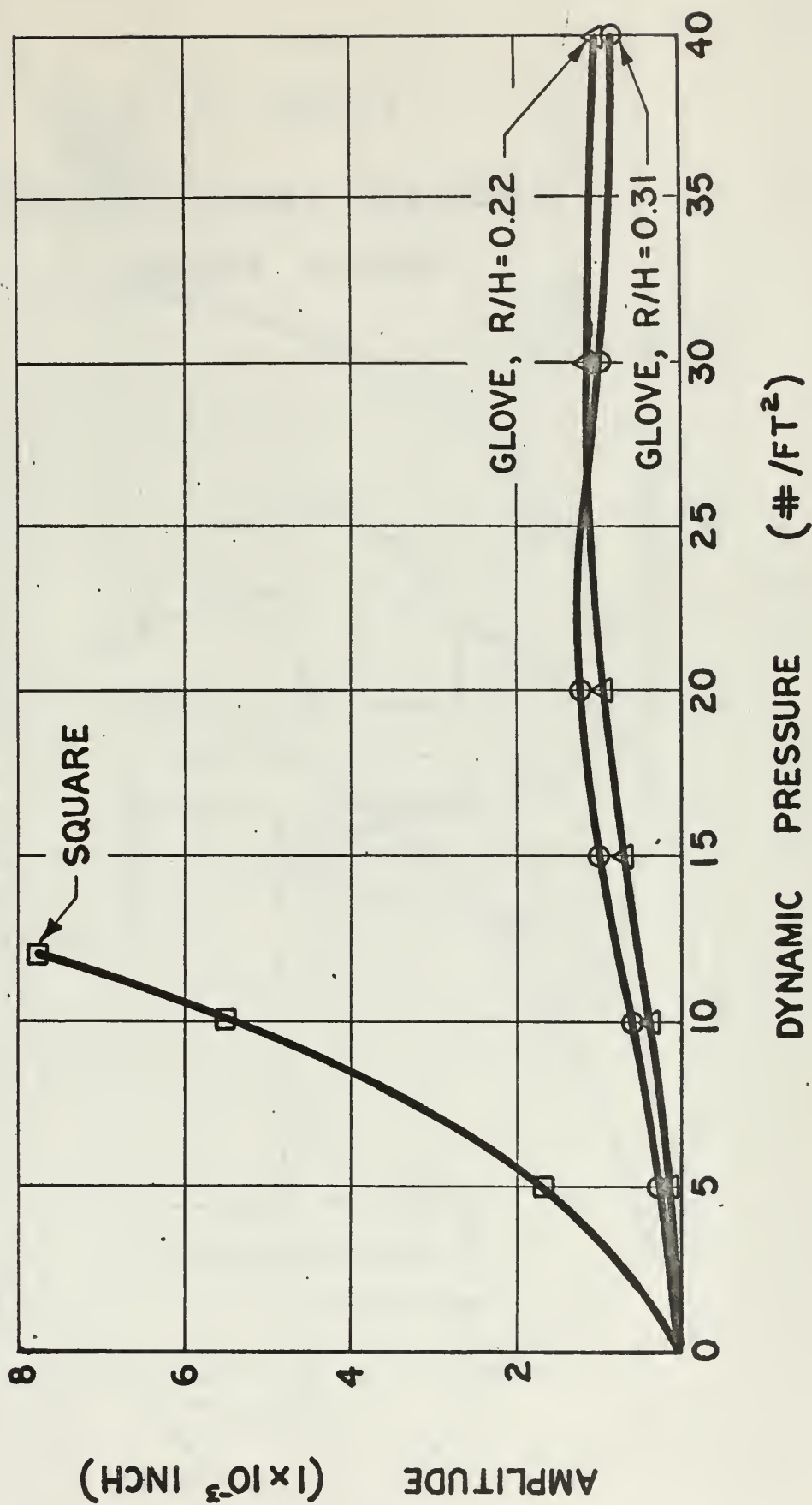


FIGURE 17
CIRCULAR CROSS SECTION
SHROUD FAIRING

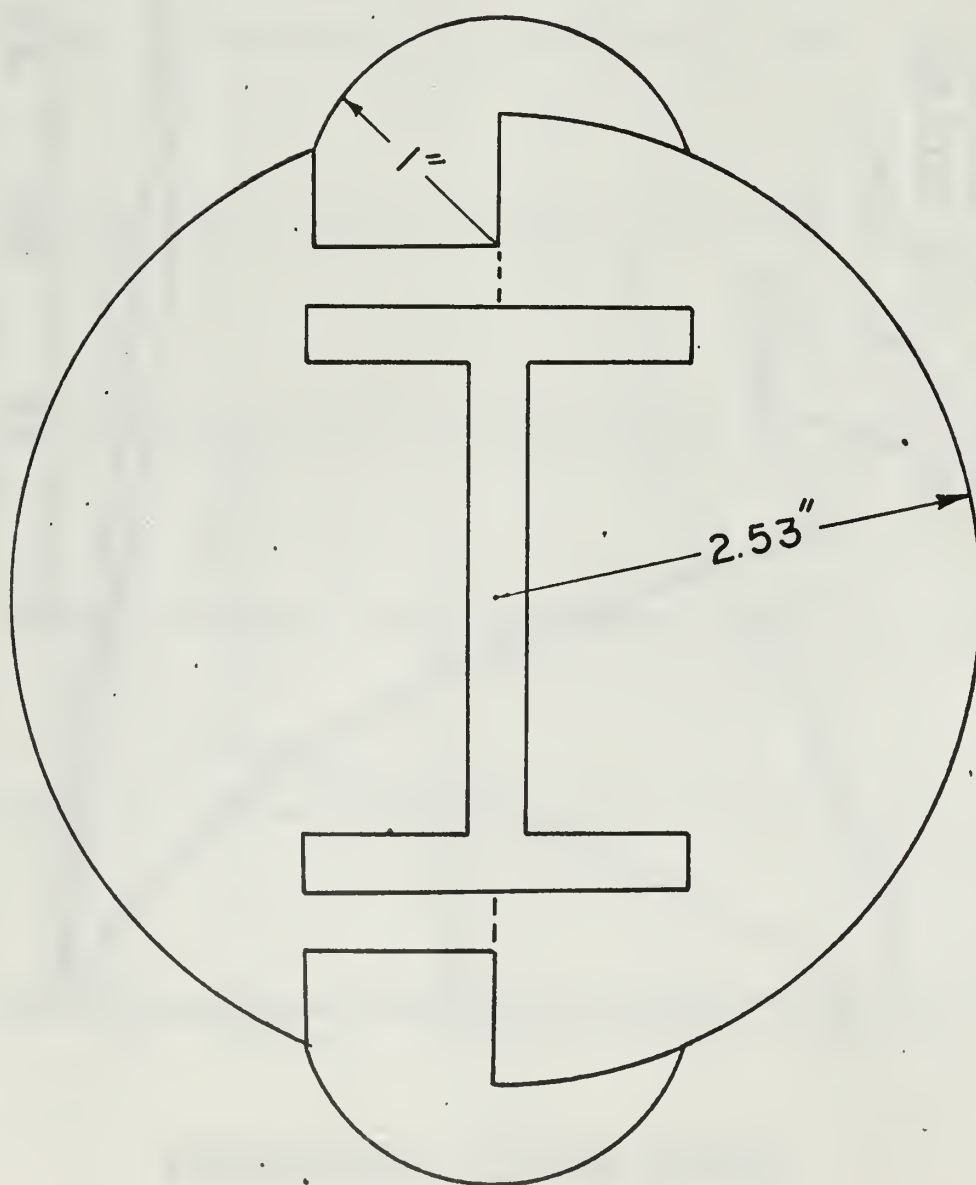


FIGURE 18
EFFECTS OF SHROUD FAIRINGS
CIRCULAR CYLINDER $\lambda_B = 3.0$ INCHES

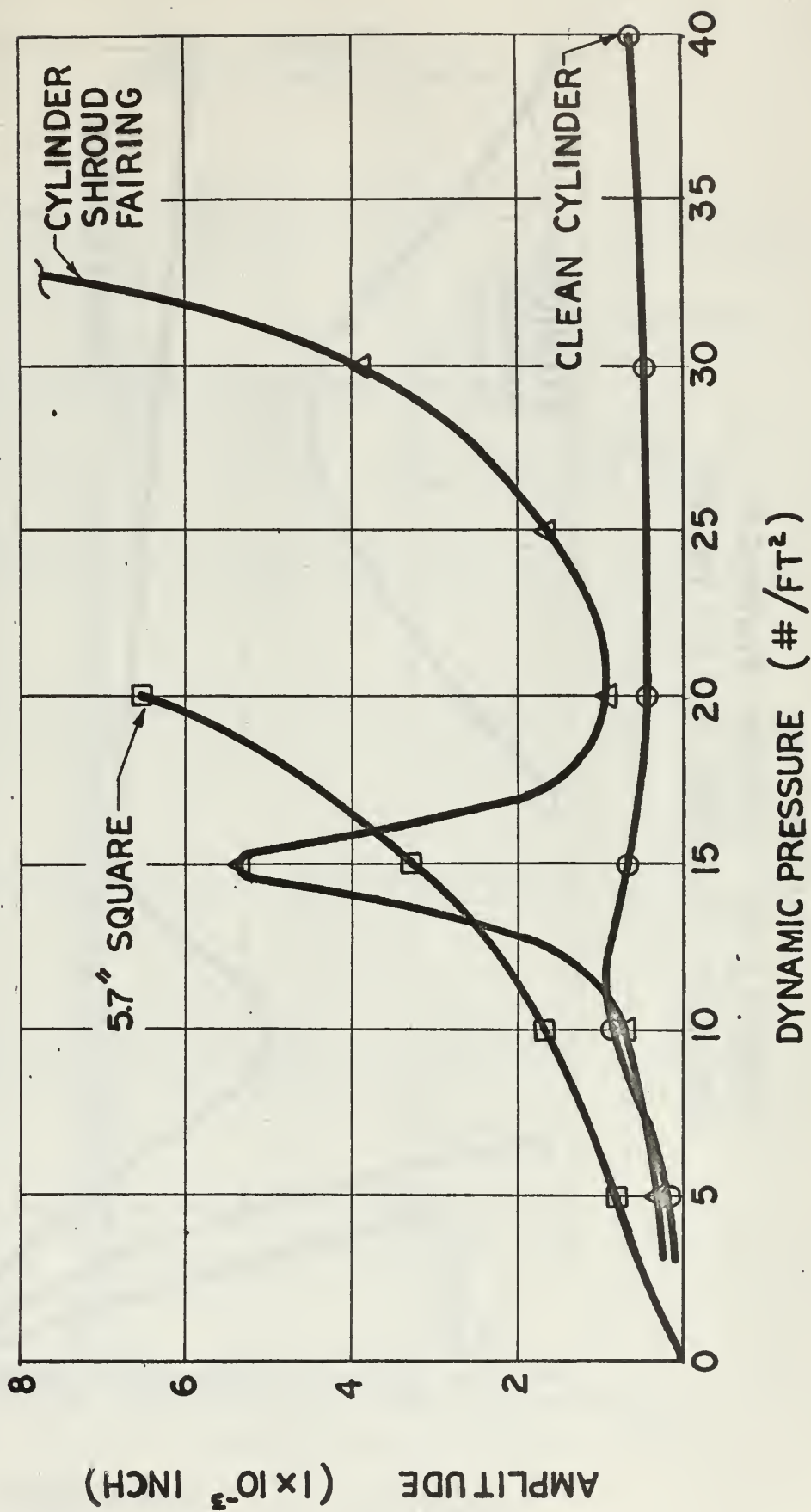


FIGURE 19
EFFECTS OF SHROUD FAIRINGS
CIRCULAR CYLINDER $\lambda_B = 6.5$ INCHES

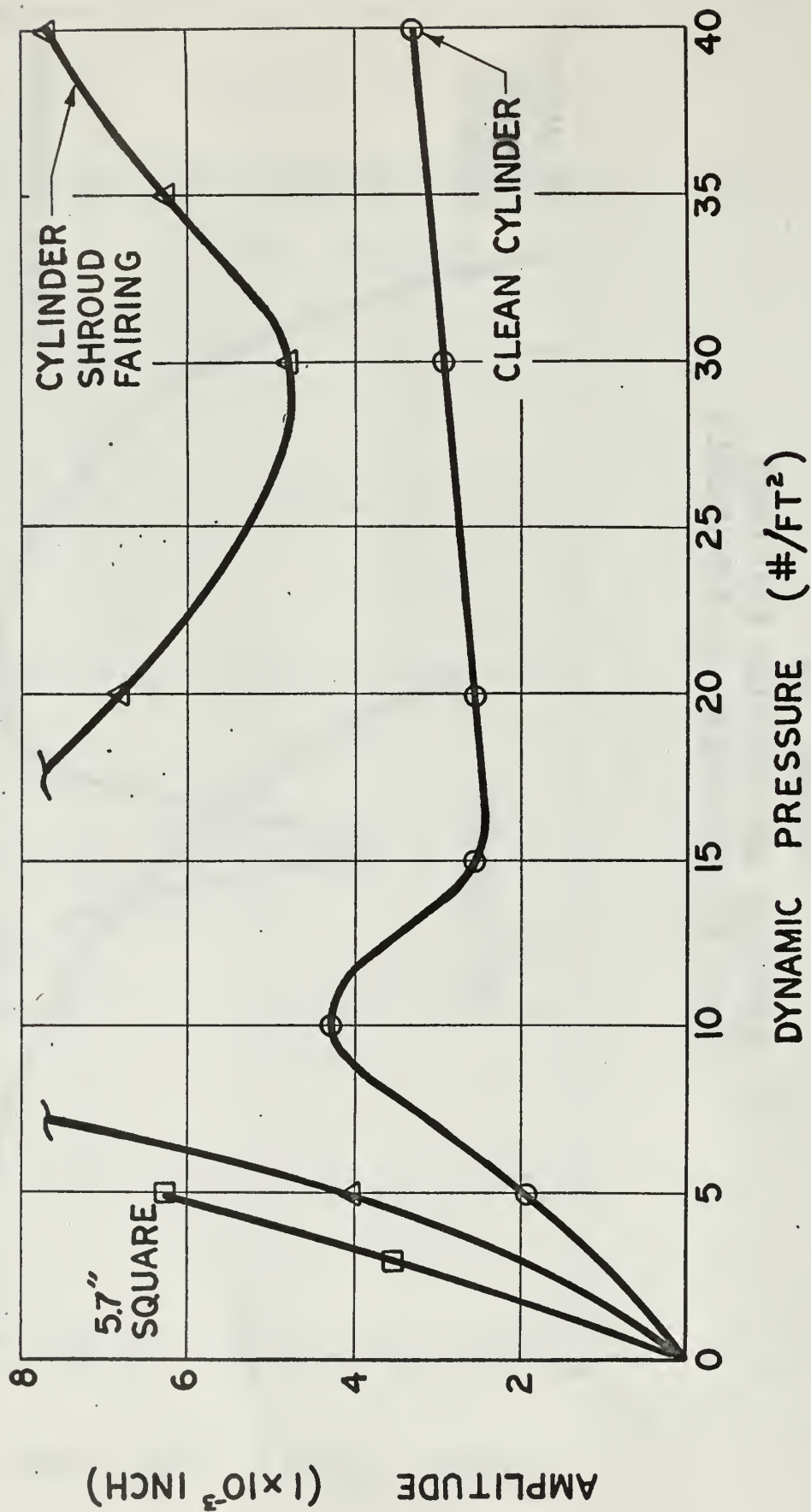


Figure 20
P.S.D. OF OUTPUT AT $q=8$ PSF

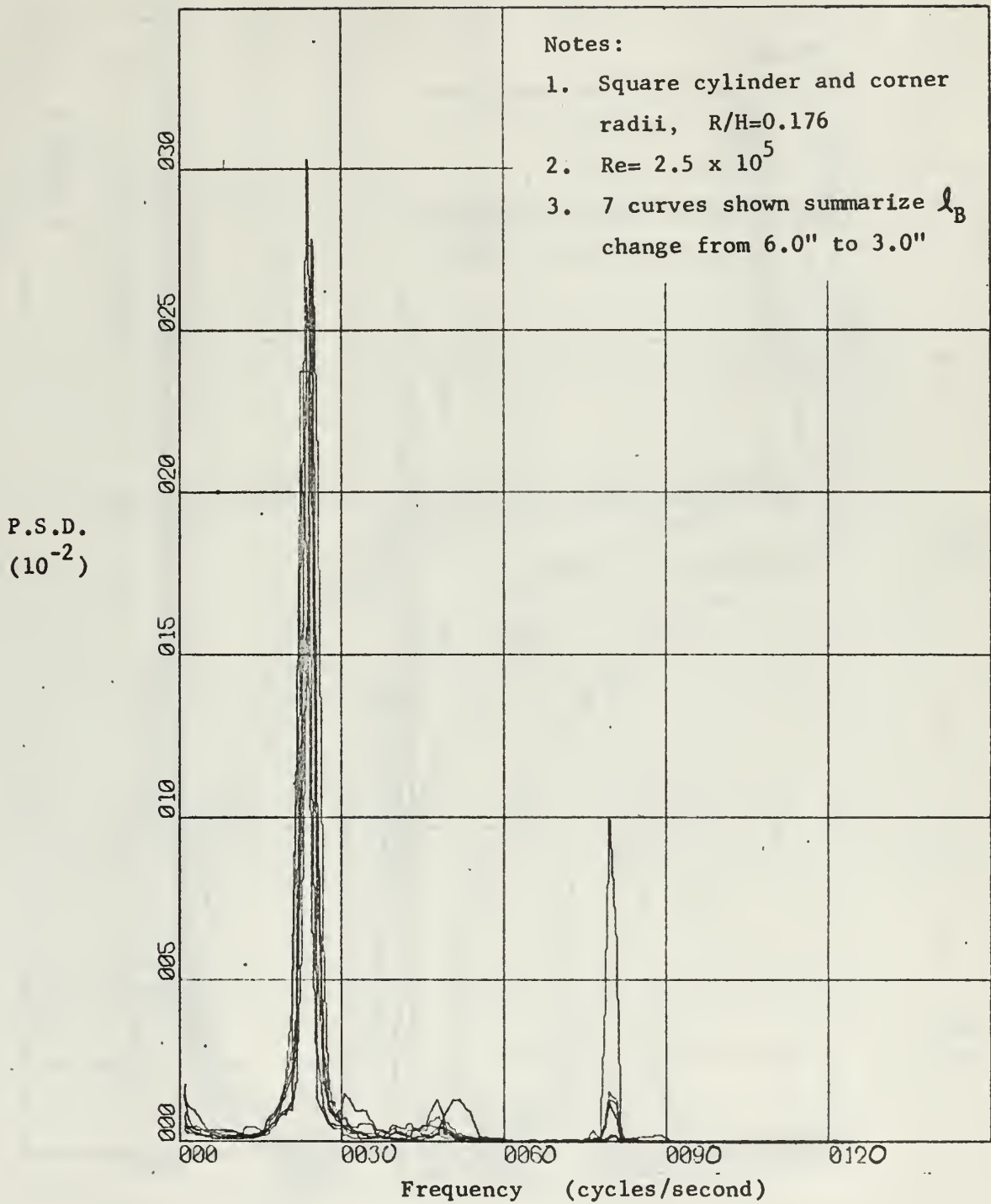


Figure 21
P.S.D. OF OUTPUT AT $q=40$ PSF

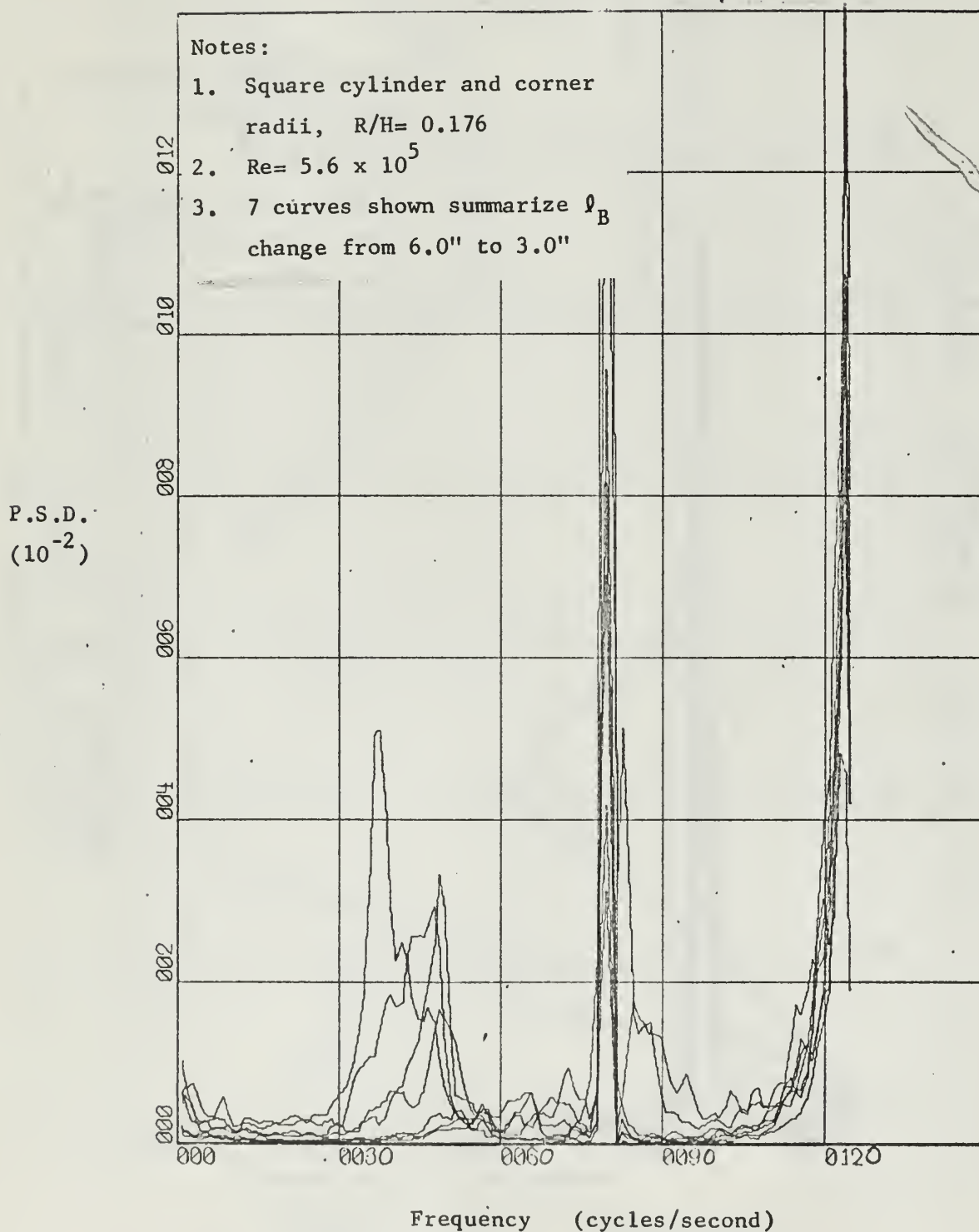


FIGURE 22
COEFFICIENT OF LIFT
EXPERIMENTAL RESULTS

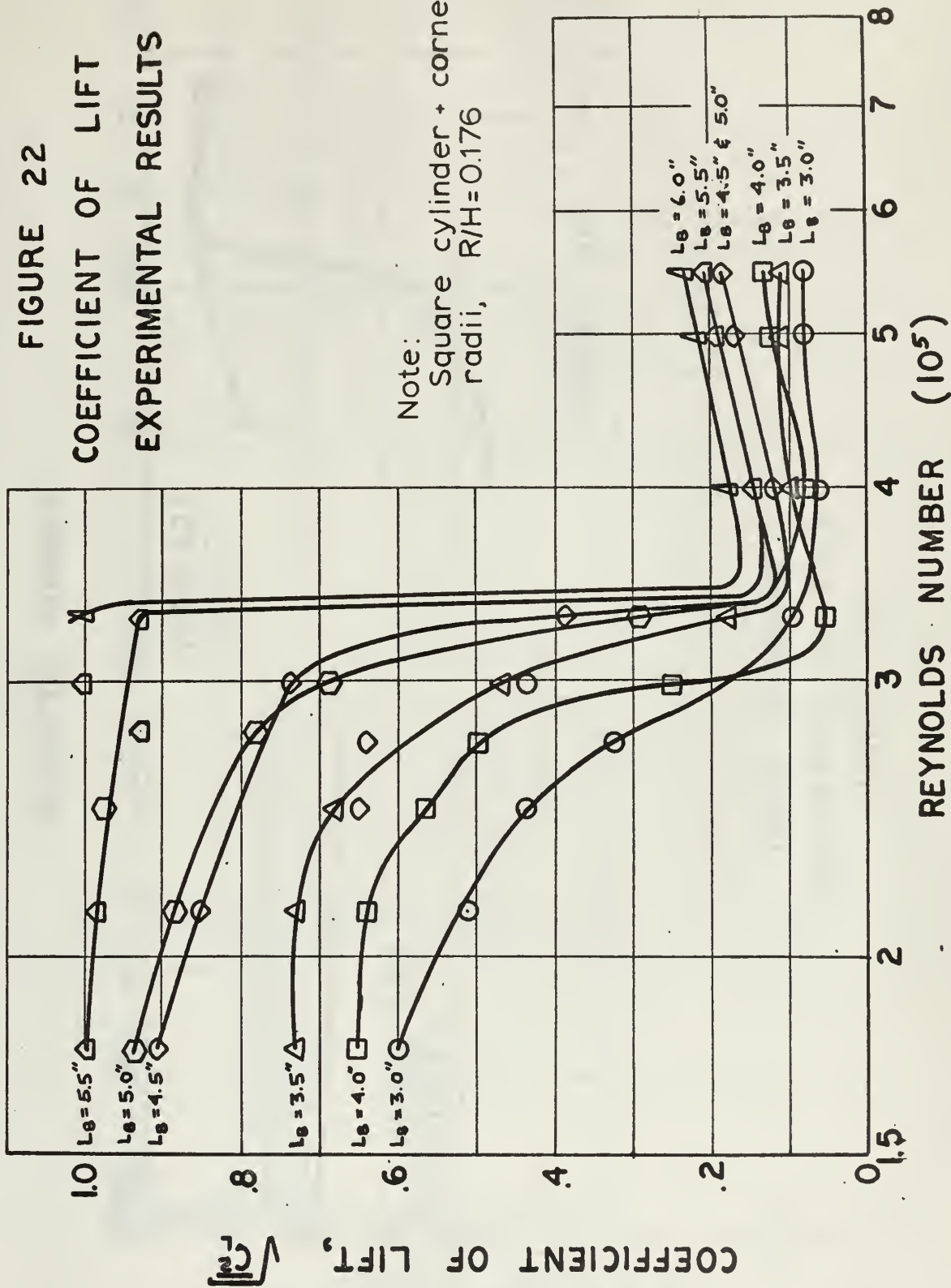


FIGURE 23
COEFFICIENT OF LIFT
DATA SUMMARY

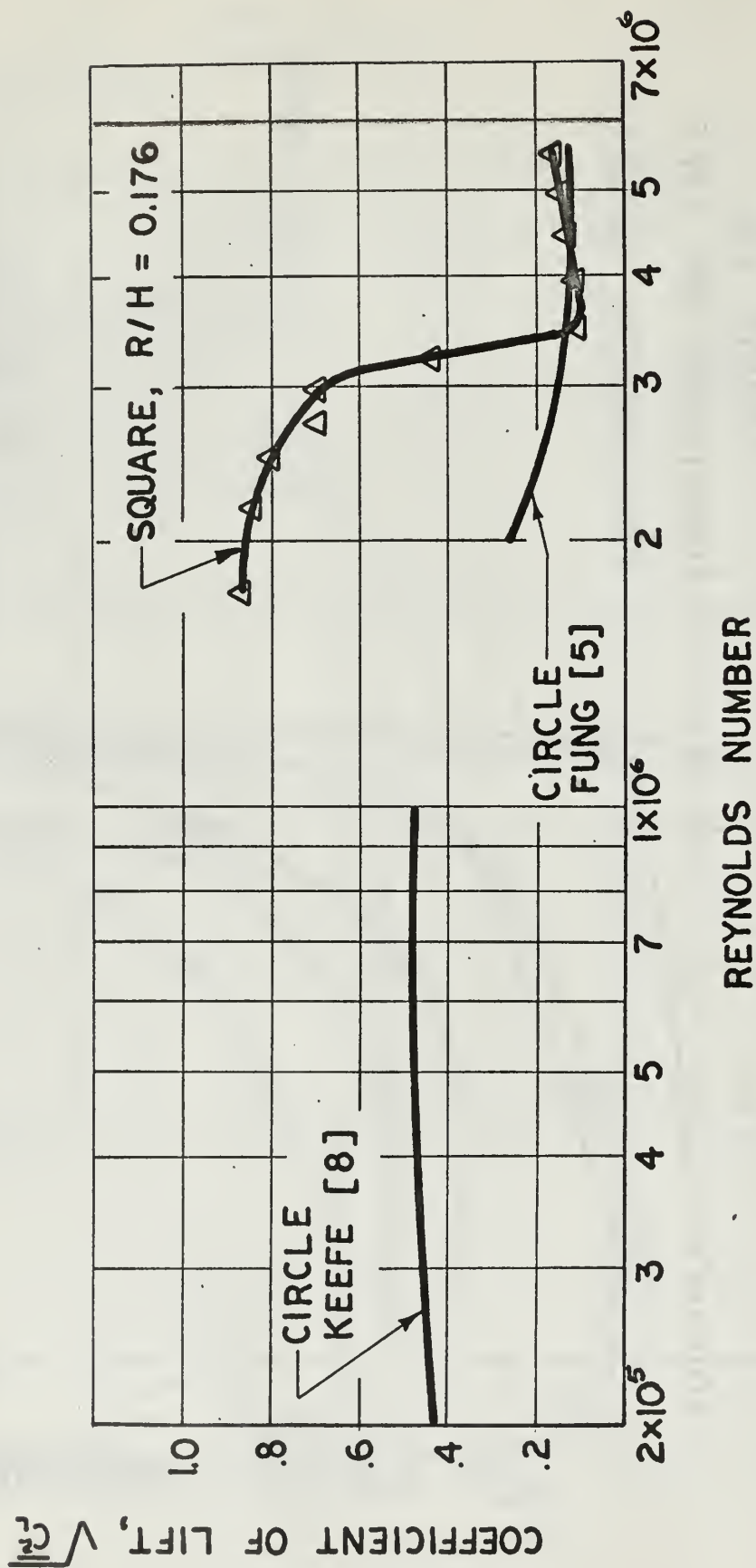


Figure 24
P.S.D. OF INPUT AT $q=8$ PSF

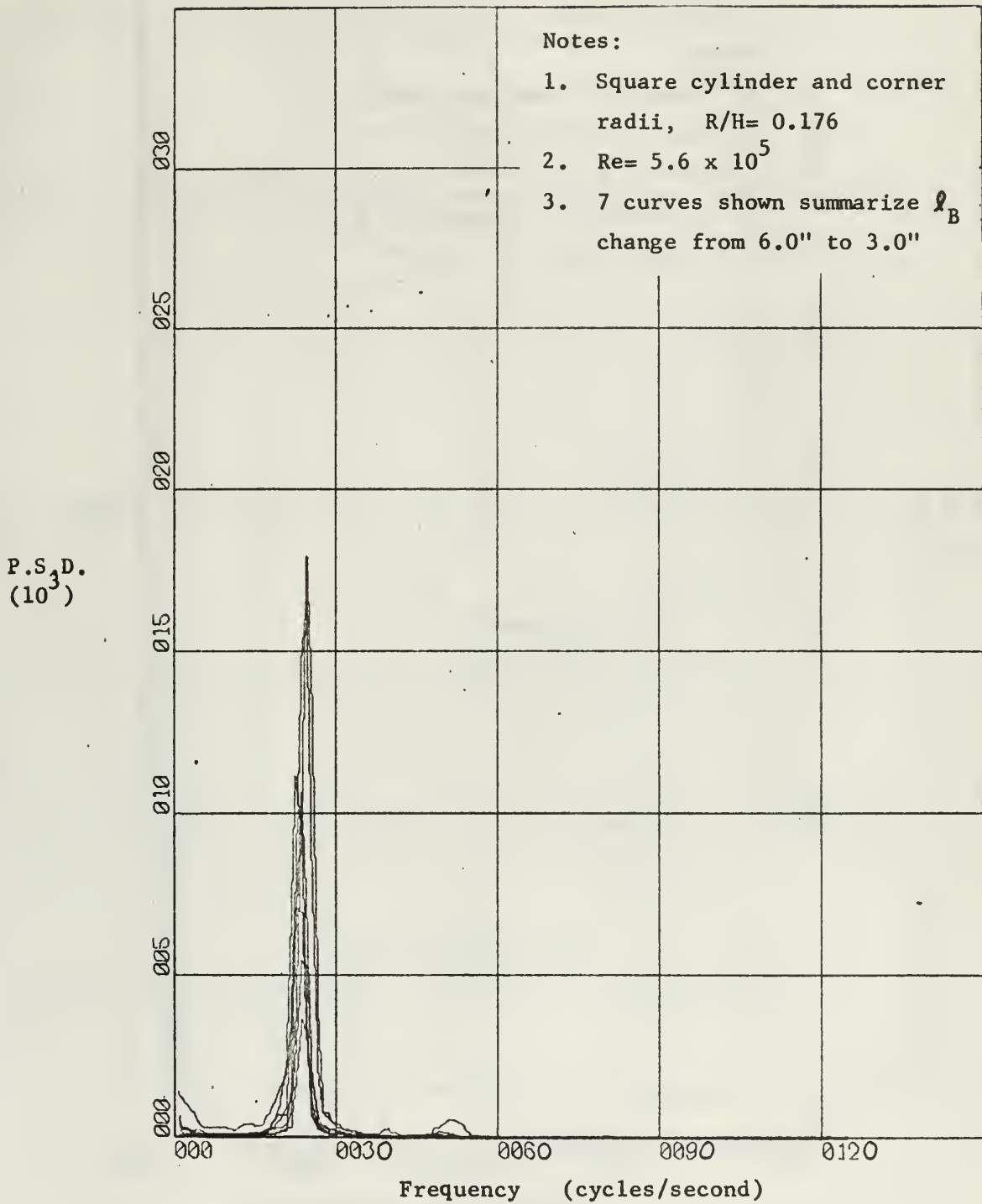


Figure 25
P.S.D. OF INPUT AT $q=40$ PSF

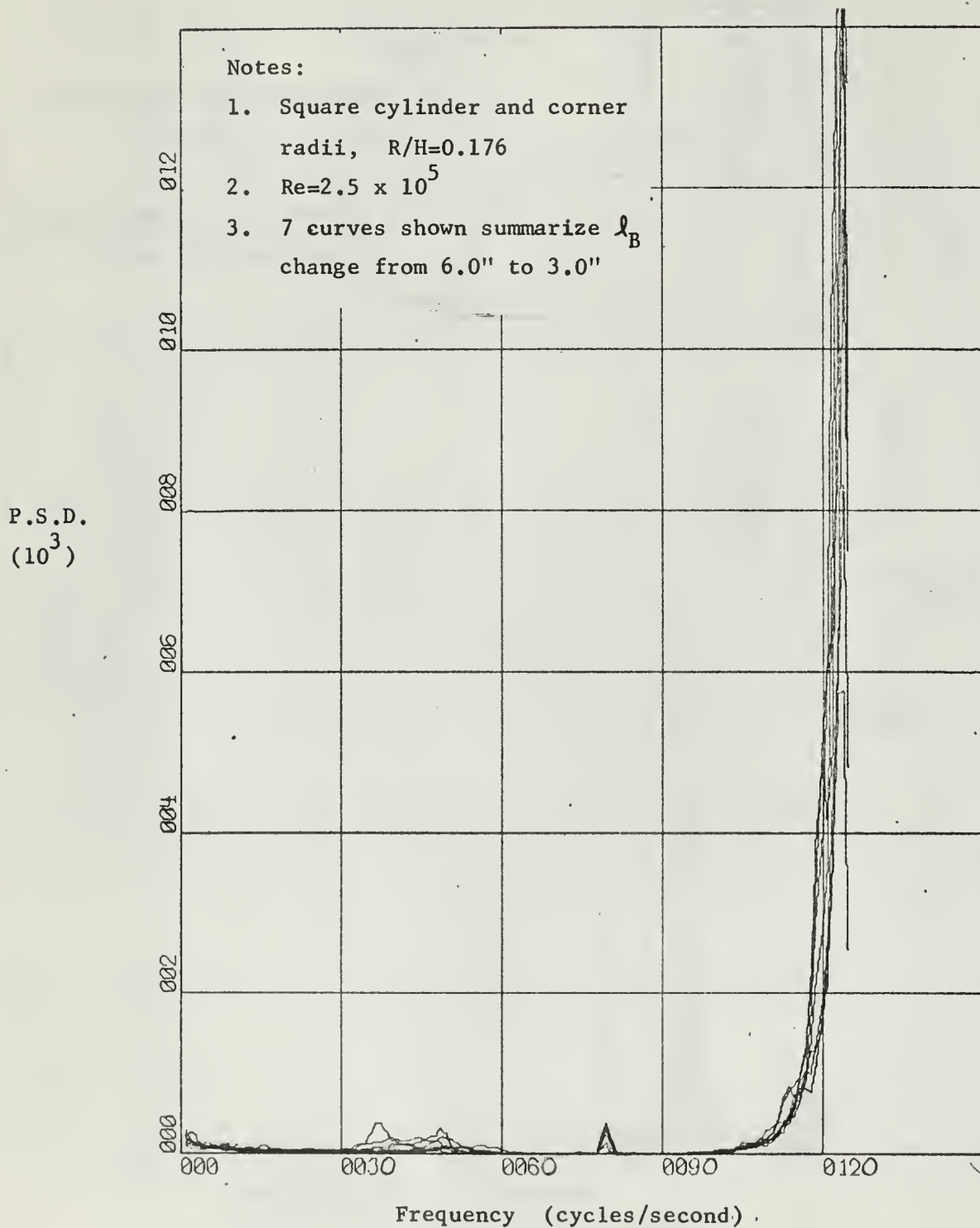
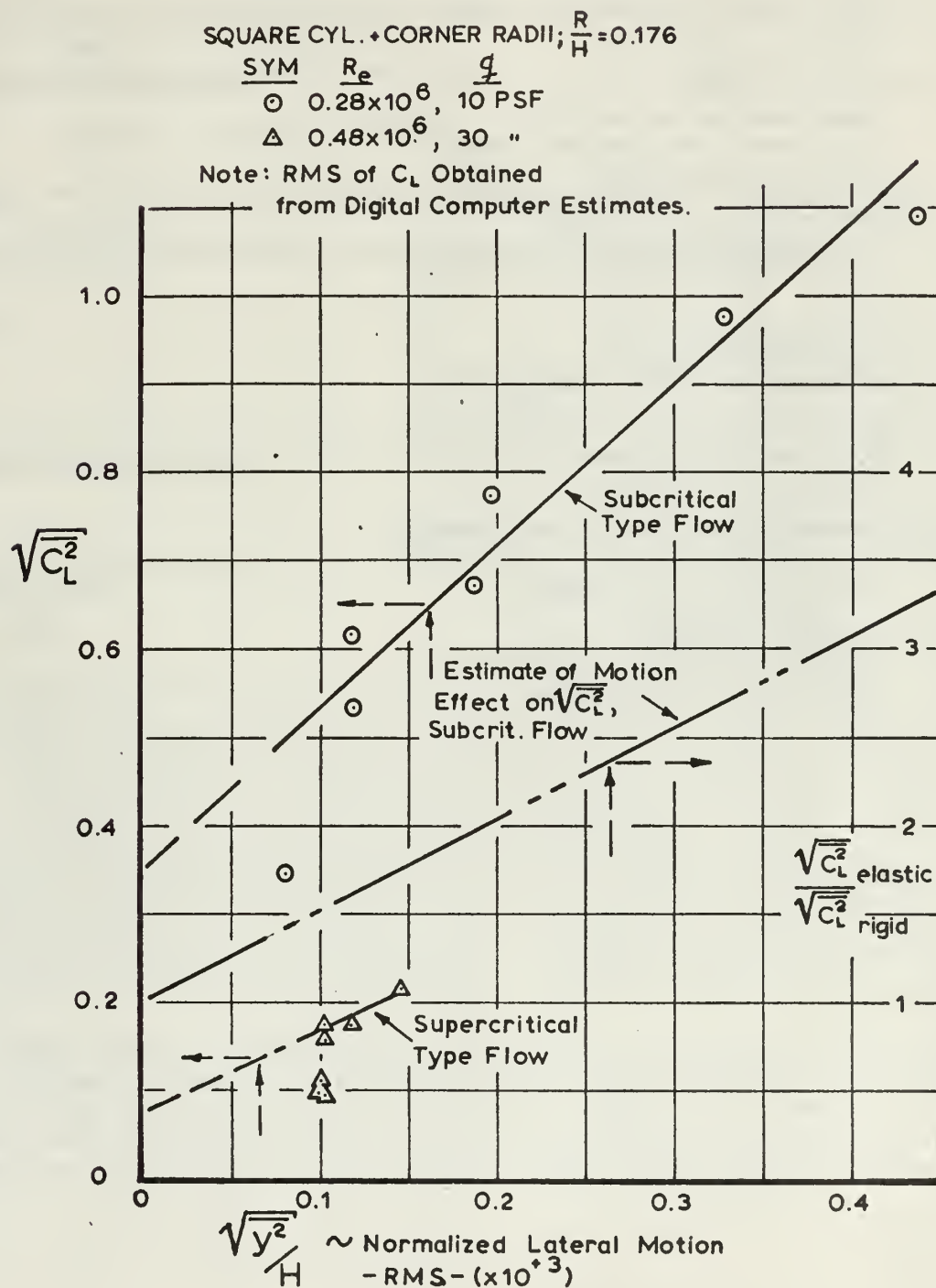


FIGURE 26 AEROELASTIC EFFECTS ON UNSTEADY LIFT



INITIAL DISTRIBUTION LIST

	No. Copies
1. Defense Documentation Center Cameron Station Alexandria, Virginia 22314	20
2. Library U. S. Naval Postgraduate School Monterey, California	2
3. Dr. L. V. Schmidt Department of Aeronautics U. S. Naval Postgraduate School Monterey, California	1
4. LT W. P. Mortenson, USN 7531 South Taft Street Seattle 78, Washington	1
5. LT R. H. Jesberg, USN 22 Nepperham Avenue Hastings on Hudson, New York	1
6. Chairman, Department of Aeronautics U. S. Naval Postgraduate School Monterey, California	1
7. Commander Naval Air Systems Command Navy Department Washington, D. C. 20360	1
8. Structures Division USN Civil Engineering Laboratory Port Hueneme, California	25

DOCUMENT CONTROL DATA - R&D

(Security classification of title, body of abstract and indexing annotation must be entered when the overall report is classified)

1. ORIGINATING ACTIVITY (Corporate author) U. S. Naval Postgraduate School Monterey, California		2a. REPORT SECURITY CLASSIFICATION Unclassified	
		2b. GROUP	
3. REPORT TITLE Aeroelastic Problems in an Antenna Vibration Project			
4. DESCRIPTIVE NOTES (Type of report and inclusive dates) Thesis			
5. AUTHOR(S) (Last name, first name, initial) Mortenson, William P. LT/USN			
6. REPORT DATE May 1966		7a. TOTAL NO. OF PAGES 60	7b. NO. OF REFS 8
8a. CONTRACT OR GRANT NO.		9a. ORIGINATOR'S REPORT NUMBER(S)	
b. PROJECT NO.			
c.		9b. OTHER REPORT NO(S) (Any other numbers that may be assigned this report)	
d.			
10. AVAILABILITY/LIMITATION NOTICES This document has been approved for public release and sale; its distribution is unlimited. Mortenson 1/6/70			
11. SUPPLEMENTARY NOTES		12. SPONSORING MILITARY ACTIVITY Naval Air Systems Command Navy Department, Washington, D. C.	
13. ABSTRACT Continued studies were made of bluff body separation and its effect upon the response of an aeroelastic model for a range of tunnel air speeds and model cross sections. The motivation for this work was the application to the antenna element vibration problem as posed in the various Wullenwebber type antenna installations operated by the United States Navy throughout the world. A retrofit configuration change was devised to significantly decrease the wind induced response of the long horizontal "boom boards". Although flow separation still exists, the character of the aerodynamic forcing function has been modified such that the energy spectra has apparently been broadened from a single dominant peak into many weaker peaks. Thus the effective total response is reduced. The digital data processing has been extended in scope due to the repeatability in signal analysis. Estimates have been made of the "two dimensional" random input forcing function using the output response in conjunction with the aeroelastic model transfer function. Reasonably good results were obtained and an estimate was made of the root mean square value of the unsteady fluctuating air load.			

14. KEY WORDS	LINK A		LINK B		LINK C	
	ROLE	WT	ROLE	WT	ROLE	WT
Bluff bodies						
Random forcing functions						
Vortex shedding						
Wullenwebber Antenna						
Strouhal						
Aeroelastic						

INSTRUCTIONS

1. **ORIGINATING ACTIVITY:** Enter the name and address of the contractor, subcontractor, grantee, Department of Defense activity or other organization (*corporate author*) issuing the report.

2a. **REPORT SECURITY CLASSIFICATION:** Enter the overall security classification of the report. Indicate whether "Restricted Data" is included. Marking is to be in accordance with appropriate security regulations.

2b. **GROUP:** Automatic downgrading is specified in DoD Directive 5200.10 and Armed Forces Industrial Manual. Enter the group number. Also, when applicable, show that optional markings have been used for Group 3 and Group 4 as authorized.

3. **REPORT TITLE:** Enter the complete report title in all capital letters. Titles in all cases should be unclassified. If a meaningful title cannot be selected without classification, show title classification in all capitals in parenthesis immediately following the title.

4. **DESCRIPTIVE NOTES:** If appropriate, enter the type of report, e.g., interim, progress, summary, annual, or final. Give the inclusive dates when a specific reporting period is covered.

5. **AUTHOR(S):** Enter the name(s) of author(s) as shown on or in the report. Enter last name, first name, middle initial. If military, show rank and branch of service. The name of the principal author is an absolute minimum requirement.

6. **REPORT DATE:** Enter the date of the report as day, month, year, or month, year. If more than one date appears on the report, use date of publication.

7a. **TOTAL NUMBER OF PAGES:** The total page count should follow normal pagination procedures, i.e., enter the number of pages containing information.

7b. **NUMBER OF REFERENCES:** Enter the total number of references cited in the report.

8a. **CONTRACT OR GRANT NUMBER:** If appropriate, enter the applicable number of the contract or grant under which the report was written.

8b, 8c, & 8d. **PROJECT NUMBER:** Enter the appropriate military department identification, such as project number, subproject number, system numbers, task number, etc.

9a. **ORIGINATOR'S REPORT NUMBER(S):** Enter the official report number by which the document will be identified and controlled by the originating activity. This number must be unique to this report.

9b. **OTHER REPORT NUMBER(S):** If the report has been assigned any other report numbers (*either by the originator or by the sponsor*), also enter this number(s).

10. **AVAILABILITY/LIMITATION NOTICES:** Enter any limitations on further dissemination of the report, other than those

imposed by security classification, using standard statements such as:

- (1) "Qualified requesters may obtain copies of this report from DDC."
- (2) "Foreign announcement and dissemination of this report by DDC is not authorized."
- (3) "U. S. Government agencies may obtain copies of this report directly from DDC. Other qualified DDC users shall request through _____."
- (4) "U. S. military agencies may obtain copies of this report directly from DDC. Other qualified users shall request through _____."
- (5) "All distribution of this report is controlled. Qualified DDC users shall request through _____."

If the report has been furnished to the Office of Technical Services, Department of Commerce, for sale to the public, indicate this fact and enter the price, if known.

11. **SUPPLEMENTARY NOTES:** Use for additional explanatory notes.

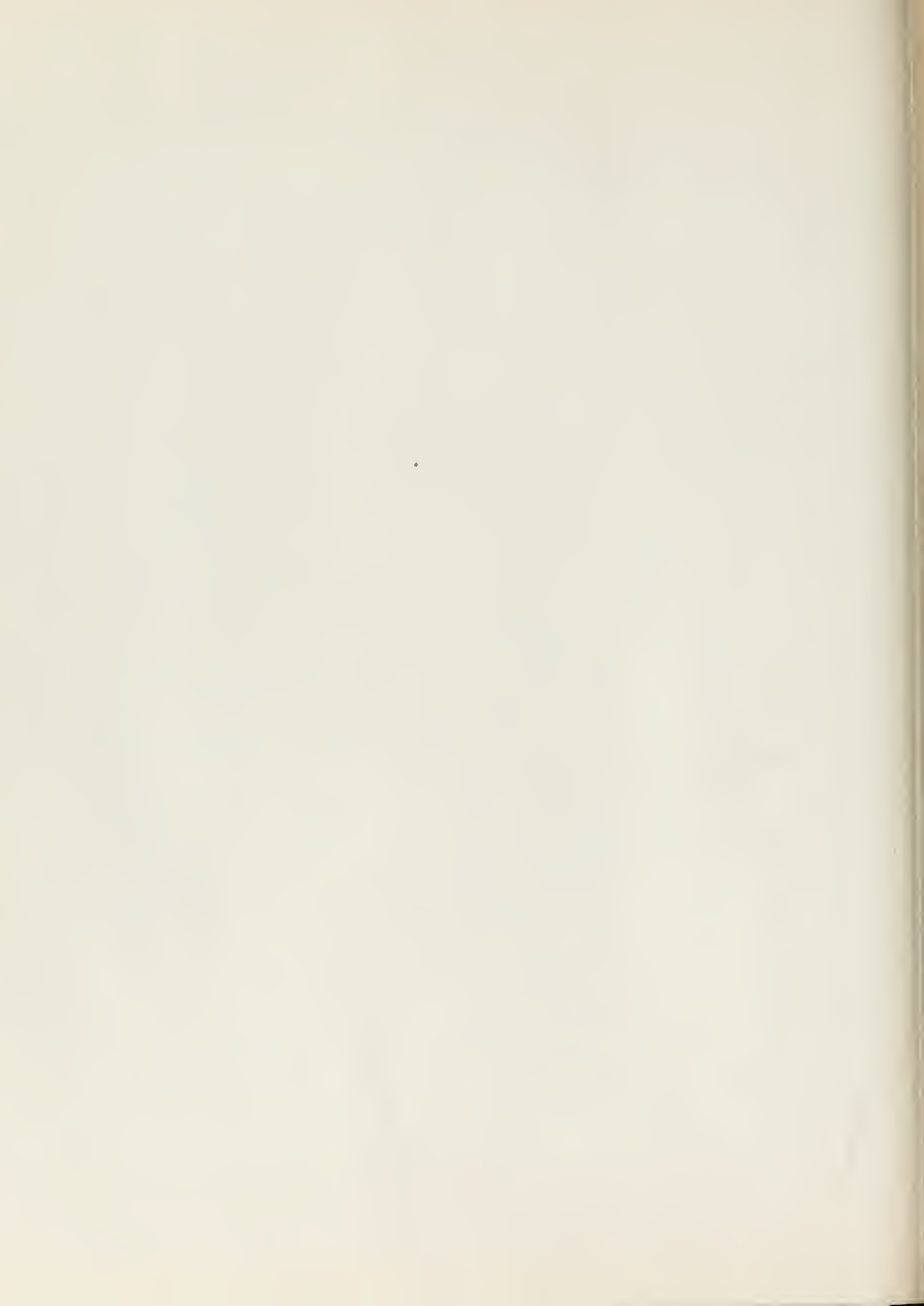
12. **SPONSORING MILITARY ACTIVITY:** Enter the name of the departmental project office or laboratory sponsoring (*paying for*) the research and development. Include address.

13. **ABSTRACT:** Enter an abstract giving a brief and factual summary of the document indicative of the report, even though it may also appear elsewhere in the body of the technical report. If additional space is required, a continuation sheet shall be attached.

It is highly desirable that the abstract of classified reports be unclassified. Each paragraph of the abstract shall end with an indication of the military security classification of the information in the paragraph, represented as (TS), (S), (C), or (U).

There is no limitation on the length of the abstract. However, the suggested length is from 150 to 225 words.

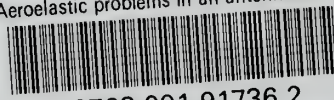
14. **KEY WORDS:** Key words are technically meaningful terms or short phrases that characterize a report and may be used as index entries for cataloging the report. Key words must be selected so that no security classification is required. Identifiers, such as equipment model designation, trade name, military project code name, geographic location, may be used as key words but will be followed by an indication of technical context. The assignment of links, roles, and weights is optional.



100

thesM8398

Aeroelastic problems in an antenna vibra



3 2768 001 91736 2

DUDLEY KNOX LIBRARY